공학박사 학위논문

Development of silver and metal oxide catalysts for direct epoxidation of propylene to propylene oxide

프로필렌의 직접산화반응을 통해 산화프로필렌을 생산하기 위한 은 및 금속산화물 촉매 개발

2019년 2월

서울대학교 대학원

화학생물공학부

이 어 진

Abstract

Development of silver and metal oxide catalysts for direct epoxidation of propylene to propylene oxide

Eo Jin Lee

School of Chemical and Biological Engineering

The Graduate School

Seoul National University

Propylene oxide accounts for a very large proportion in the petrochemical industry and more than 10% of the total propylene production is used for the production of propylene oxide. Propylene oxide is used as a raw material for the production of Polyether Polyol and Propylene Glycol, which are raw materials of polyurethane. With the growth of polyurethane industry, the demand of propylene oxide is also steadily increasing. Commercially, propylene oxide is produced though indirect processes such as chlorohydrin process and Halcon process. However, these processes have many drawbacks from environmental and economical viewpoints. Chlorohydrin process has shortcomings in a sense that it produces large amount of chlorinated by-products and waste salts. Halcon process also has a problem, because it requires additional treatment steps to separate propylene oxide and co-products (styrene and t-butylalcohol). On the other hand, HPPO (hydrogen peroxide-propylene oxide) process, which produces propylene oxide using hydrogen peroxide, has been developed to replace the commercial processes. Because of high cost of

hydrogen peroxide, however, this process has been restricted in industry. Therefore, direct preparation of propylene oxide from propylene and oxygen has attracted much attention as a cheap and green chemical process. It has been reported that undesired complete oxidation ($C_3H_6 + 9/2O_2 \rightarrow 3CO_2 + 3H_2O$, $\Delta G = -1957.43$ kJ/mol) occurs together with selective partial oxidation of propylene to propylene oxide ($C_3H_6 + 1/2O_2 \rightarrow 3C_3H_6O$, $\Delta G = -88.49$ kJ/mol) in the direct preparation of propylene oxide from propylene and oxygen. For this reason, selectivity for propylene oxide in the direct epoxidation of propylene is thermodynamically limited. It is well known that silver catalyst supported on α-alumina has been used in the direct epoxidation of ethylene to ethylene oxide. In the direct epoxidation of propylene to propylene oxide, however, the catalyst showed a very low activity to propylene oxide. This is explained by the fact that allylic C-H bond energy (77 kcal/mol) of propylene is lower than vinylic C-H bond energy (112 kcal/mol) of ethylene. For this reason, hydrogen abstraction of propylene, which is the reaction of allylic hydrogen and adsorbed oxygen to form H_2O and CO_2, is more favorable than that of ethylene. As a result, selectivity for propylene oxide over the same catalyst is very low compared to selectivity for ethylene oxide. Therefore, many researches have focused on the development of an appropriate catalyst for the direct epoxidation of propylene to propylene oxide.

There are two reaction pathways in the oxidation reaction of propylene. Propylene oxide is formed by partial oxidation of C=C π bond in propylene with oxygen adsorbed on the silver active site. On the other hand, H_2O and CO_2 are formed by complete oxidation of allylic hydrogen (C-H) in propylene with oxygen adsorbed on the silver active site. These imply that electronic property of adsorbed oxygen species should be changed more electrophilic in order to improve the selectivity for propylene oxide. In this work, in order to change the electronic

property of adsorbed oxygen, promotors of molybdenum oxide and tungsten oxide were introduced into the silver catalyst.

A series of Ag-(x)Mo-(5-x)W/ZrO_2 (x = 5, 3.75, 2.50, 1.25, and 0) catalysts with different molybdenum content (x, wt%) were prepared by a slurry method. The effect of molybdenum content of Ag-(x)Mo-(5-x)W/ZrO_2 catalysts on the catalytic performance in the direct epoxidation of propylene to propylene oxide was investigated. It was found that binding energy shift of Ag $3d_{5/2}$ of the Ag-(x)Mo-(5-x)W/ZrO_2 catalysts was different depending on molybdenum content. In the direct epoxidation of propylene to propylene oxide, selectivity for propylene oxide showed a volcano-shaped trend with respect to molybdenum content. Experimental results revealed that selectivity for propylene oxide increased with increasing binding energy shift of Ag $3d_{5/2}$ of the Ag-(x)Mo-(5-x)W/ZrO_2 catalysts. Thus, electronic state of silver of Ag-(x)Mo-(5-x)W/ZrO_2 catalysts modified by molybdenum and tungsten promotors played a crucial role in determining the catalytic performance in the direct epoxidation of propylene to propylene oxide.

In an attempt to develop an efficient catalyst, direct epoxidation of propylene has been investigated over a number of catalysts based on silver metal supported on various materials such as alkali-earth metal oxide, α-Al_2O_3, and SiO_2. It has been reported that production of propylene oxide through propylene epoxidation is influenced by physicochemical properties of supporting materials such as crystalline phase or acid/base properties. ZrO_2 is known to exhibit the characteristic physicochemical properties as a supporting material. It has been also reported that the physicochemical properties of ZrO_2 can be controlled by changing ZrO_2 preparation method. In this work, in order to elucidate the effect of physicochemical properties of ZrO_2 support on the production of propylene oxide, Ag-(Mo-W)/ZrO_2 (pH X) catalysts were prepared with a variation of pH (X) for preparing ZrO_2

support.

A series of ZrO_2 (pH X) (X = 3, 6, 10, 12, and 14) supports were prepared by a precipitation method with a variation of pH value (pH X) of ZrO_2 solution. Ag-(Mo-W)/ZrO_2 (pH X) (X = 3, 6, 10, 12, and 14) catalysts were then prepared by a slurry method for use in the direct epoxidation of propylene to propylene oxide with molecular oxygen. The effect of pH value of ZrO_2 solution on the catalytic performance and physicochemical property of the catalysts was investigated. Experimental results revealed that physicochemical properties of Ag-(Mo-W)/ZrO_2 (pH X) catalysts were strongly influenced by pH value of ZrO_2 solution. It was found that the fraction of monoclinic phase showed a volcano-shaped trend with respect to pH value of ZrO_2 solution. It was also revealed that the ratio of acidity/basicity showed a volcano-shaped trend with respect to pH value of ZrO_2 solution. In the direct epoxidation of propylene to propylene oxide, selectivity for propylene oxide was well correlated with the fraction of monoclinic phase and the ratio of acidity/basicity of the catalysts. Selectivity for propylene oxide increased with increasing the ratio of monoclinic phase and the ratio of acidity/basicity of the catalysts. Therefore, ZrO_2 crystalline phase and acid/base property of the catalysts played key roles in determining the catalytic performance of Ag-(Mo-W)/ZrO_2 (pH X) catalysts in the direct epoxidation of propylene to propylene oxide.

Direct epoxidation of propylene has been mainly studied over Ag-based catalyst system. However, it is known that commercial Ag-based catalysts suffer from deactivation in the oxidation reaction, because silver particles are sintered during the oxidation reaction. Ag-based catalysts also have a disadvantage in the direct epoxidation in a sense that high silver loading is required for high catalytic activity, and thus, high silver content in the catalyst may cause a silver sintering during the long-term operation. For these reasons, many researches have been

focused on the metal oxide catalyst system in the direct epoxidation of propylene to propylene oxide. In this work, in order to replace the Ag-based catalyst in the direct epoxidation of propylene, tungsten oxide catalysts supported on various supports (ZrO_2, $CeZrO_2$, and CeO_2) were prepared.

$Ce_{0.05}Zr_{0.95}O_2$ support (denoted as CZ) was prepared by a precipitation method for use a support for tungsten oxide catalyst. For comparison, ZrO_2 (denoted as Z) and CeO_2 (denoted as C) supports were also prepared by a precipitation method, respectively. Tungsten oxide catalysts on ZrO_2, $Ce_{0.05}Zr_{0.95}O_2$, and CeO_2 supports were then prepared by a wetness impregnation method for use in the direct epoxidation of propylene to propylene oxide. Experimental results revealed that WO_x/Z catalyst exhibited the highest selectivity for propylene oxide. However, very low propylene conversion was observed over WO_x/Z catalyst, leading to low yield for propylene oxide. On the other hand, WO_x/C catalyst exhibited higher conversion of propylene than WO_x/Z, but WO_x/C showed low selectivity for propylene oxide. Among the catalysts, WO_x/CZ catalyst with moderate reduction ability and ratio of acidity/basicity exhibited the suitable conversion of propylene and selectivity for propylene oxide. Thus, reduction ability and ratio of acidity/basicity played a key role in determining the catalytic performance in the direct epoxidation of propylene to propylene oxide over ceria and zirconia-supported tungsten oxide catalyst.

Keywords: Direct epoxidation, Propylene oxide, Silver catalyst, Tungsten oxide catalyst

Student Number: 2016-30235

Contents

Chapter 1. Introduction 1

1.1. Propylene oxide (PO) 1

1.2. Two reaction pathways for oxidation of propylene 3

1.3. Difference between ethylene and propylene in the oxidation reaction 5

1.4. DAM (dipped adcluster model) theory 7

Chapter 2. Direct epoxidation of propylene to propylene oxide with molecular oxygen over Ag-(x)Mo-(5-x)W/ZrO_2 catalysts 9

2.1. Introduction 9

2.2. Experimental 11

2.2.1. Preparation of catalysts 11

2.2.2. Characterizations 13

2.2.3. Catalyst reaction tests 14

2.3. Results and discussion 15

2.3.1. Characterization of Ag-(x)Mo-(5-x)W/ZrO_2 catalysts 15

2.3.2. Catalytic performance in the direct epoxidation of propylene to propylene oxide 19

Chapter 3. Direct epoxidation of propylene to propylene oxide over Ag-(Mo-W)/ZrO_2 catalysts: Effect of pH in the preparation of ZrO_2 support by a precipitation method 29

3.1. Introduction 29

3.2. Experimental 32

3.2.1. Preparation of catalysts 32

3.2.2. Characterizations 35

3.2.3. Catalyst reaction tests 37

3.3. Results and discussion 38

3.3.1. Textural property and morphology of Ag-(Mo-W)/ZrO_2 (pH X) catalysts 38
3.3.2. NH_3-TPD and CO_2-TPD analyses of Ag-(Mo-W)/ZrO_2 (pH X) catalysts 41
3.3.3. Catalytic performance in the direct epoxidation of propylene to propylene oxide 43
3.3.4. Correlations between catalytic performance and catalytic property 44

Chapter 4. Propylene epoxidation by oxygen over tungsten oxide supported on ceria-zirconia ..56

4.1. Introduction 56
4.2. Experimental 59
4.2.1. Preparation of catalysts 59
4.2.2. Characterizations 62
4.2.3. Catalyst reaction tests 64
4.3. Results 65
4.3.1. Catalytic performance of ceria & zirconia-supported tungsten oxides 65
4.3.1.1. Effect of $WO_x/Ce_xZr_{1-x}O_2$ catalyst on the propylene epoxidation 65
4.3.1.2. Effect of (X wt%) $WO_x/Ce_{0.05}Zr_{0.95}O_2$ catalyst on the propylene epoxidation 66
4.3.1.3. Effect of (10 wt%) $WO_x/Ce_{0.05}Zr_{0.95}O_2$-X ^oC catalyst on the propylene epoxidation 66
4.3.2. Characterization of ceria & zirconia-supported tungsten oxides 68
4.3.2.1. Textural properties and morphology of catalysts 68
4.3.2.2. H_2-TPR of catalysts 70
4.3.2.3. Acidity & basicity of catalysts 72
4.3.2.4 Catalytic activity in the propylene epoxidation by oxygen 73
4.4. Discussion 75

Chapter 5. Conclusions 91

Bibliography.....94

초　　록.....98

List of Tables

Table 2-1. Physicochemical properties and XPS results of Ag-(x)Mo-(5-x)W/ZrO_2 (x = 5, 3.75, 2.50, 1.25, and 0) catalysts 21

Table 3-1. Textural properties of Ag-(Mo-W)/ZrO_2 (pH X) (X = 3, 6, 10, 12, and 14) catalysts 45

Table 3-2. Fraction of monoclinic phase of Ag-(Mo-W)/ZrO_2 (pH X) (X = 3, 6, 10, 12, and 14) catalysts 46

Table 3-3. Acidity, basicity, and ratio of acidity/basicity of Ag-(Mo-W)/ZrO_2 (pH X) (X = 3, 6, 10, 12, and 14) catalysts 47

Table 4-1. Textural properties of WO_x/Z, WO_x/CZ, and WO_x/C catalysts 78

Table 4-2. H_2 consumption of ZrO_2, $CeZrO_2$, and CeO_2 supports and WO_x/Z, WO_x/CZ, and WO_x/C catalysts 79

Table 4-3. Acidity, basicity, and ratio of acidity/basicity of WO_x/Z, WO_x/CZ, and WO_x/C catalysts 80

Table 4-4. Catalytic performance of ZrO_2, $CeZrO_2$, and CeO_2 supports and WO_x/Z, WO_x/CZ, and WO_x/C catalysts 81

List of Figures

Fig. 1-1. Scheme for propylene oxide commercial production process. 2

Fig. 1-2. Two reaction pathways for oxidation of propylene..... 4

Fig. 1-3. Difference between ethylene and propylene in the oxidation reaction 6

Fig. 1-4. DAM (dipped adcluster model) theory mechanism 8

Fig. 2-1. Preparation procedure for Ag-(x)Mo-(5-x)W/ZrO_2 (x = 5, 3.75, 2.50, 1.25, and 0) catalysts 12

Fig. 2-2. XRD patterns of Ag-(x)Mo-(5-x)W/ZrO_2 (x = 5, 3.75, 2.50, 1.25, and 0) catalysts..... 22

Fig. 2-3. HR-TEM and SEM-EDX mapping images of Ag-(3.75)Mo-(1.25)W/ZrO_2 catalyst..... 23

Fig. 2-4. SEM-EDX mapping images of reused Ag-(3.75)Mo-(1.25)W/ZrO_2 catalyst..... 24

Fig. 2-5. XPS spectra of Ag $3d_{5/2}$ and Ag $3d_{3/2}$ of Ag-(x)Mo-(5-x)W/ZrO_2 (x = 5, 3.75, 2.50, 1.25, and 0) catalysts..... 25

Fig. 2-6. Catalytic performance of Ag-(x)Mo-(5-x)W/ZrO_2 (x = 5, 3.75, 2.50, 1.25, and 0) catalysts with time on stream in the direct epoxidation of propylene to propylene oxide at 460 ºC..... 26

Fig. 2-7. Reusability test result for direct epoxidation of propylene to propylene oxide over Ag-(3.75)Mo-(1.25)W/ZrO2 catalyst..... 27

Fig. 2-8. **A correlation between selectivity for propylene oxide and binding energy shift of Ag $3d_{5/2}$ of Ag-(x)Mo-(5-x)W/ZrO_2 (x = 5, 3.75, 2.50, 1.25, and 0) catalysts with reference to Ag-(5)W/ZrO_2 ..... 28**

Fig. 3-1. **Preparation procedure for ZrO_2 (pH X) (X = 3, 6, 10, 12, and 14) supports and Ag-(x)Mo-(5-x)W/ZrO_2 (x = 5, 3.75, 2.50, 1.25, and 0) catalysts 34**

Fig. 3-2. **FE-SEM images of Ag-(Mo-W)/ZrO_2 (pH X) (X = 3, 10, and 14) catalysts 48**

Fig. 3-3. **SEM-EDX mapping images of Ag-(Mo-W)/ZrO_2 (pH 10) catalyst 49**

Fig. 3-4. **XRD patterns of ZrO_2 (pH X) (X = 3, 6, 10, 12, and 14) supports 50**

Fig. 3-5. **XRD patterns of Ag-(Mo-W)/ZrO_2 (pH X) (X = 3, 6, 10, 12, and 14) catalysts 51**

Fig. 3-6. **NH_3-TPD profiles of Ag-(Mo-W)/ZrO_2 (pH X) (X = 3, 6, 10, 12, and 14) catalysts 52**

Fig. 3-7. **CO_2-TPD profiles of Ag-(Mo-W)/ZrO_2 (pH X) (X = 3, 6, 10, 12, and 14) catalysts 53**

Fig. 3-8. **Propylene conversion and propylene oxide selectivity with time on stream in the direct epoxidation of propylene over Ag-(Mo-W)/ZrO_2 (pH X) (X = 3, 6, 10, 12, and 14) catalysts 54**

Fig. 3-9. **Correlations between selectivity for propylene oxide and fraction of monoclinic phase, and between selectivity for propylene oxide and ratio of acidity/basicity of the catalysts 55**

Fig. 4-1. Preparation procedure for ZrO_2, $CeZrO_2$, and CeO_2 supports and WO_x/ZrO_2, $WO_x/CeZrO_2$, and WO_x/CeO_2 catalysts 61

Fig. 4-2. Catalytic performance of the $WO_x/Ce_xZr_{1-x}O_2$ (x =0.05, 0.1, 0.2, 0.3, 0.4, and 0.5) catalysts in the propylene epoxidation by oxygen 82

Fig. 4-3. Catalytic performance of the (X wt%) $WO_x/Ce_{0.05}Zr_{0.95}O_2$ (X= 1.8, 3.6, 4.8, 7.0, 10.0, and 13.6) catalysts in the propylene epoxidation by oxygen 83

Fig. 4-4. Catalytic performance of the (10 wt%) $WO_x/Ce_{0.05}Zr_{0.95}O_2$-X (X= 500, 600, 700, 800, and 900 °C) catalysts in the propylene epoxidation by oxygen..... 84

Fig. 4-5. FE-SEM and EDX mapping images of WO_x/CZ catalyst 85

Fig. 4-6. (a) XRD patterns of ZrO_2, $Ce_{0.05}Zr_{0.95}O_2$, and CeO_2 supports, and (b) XRD patterns of WO_x/Z, WO_x/CZ, and WO_x/C catalysts..... 86

Fig. 4-7. (a) TPR profiles of ZrO_2, $Ce_{0.05}Zr_{0.95}O_2$, and CeO_2 supports, and (b) TPR profiles WO_x/Z, WO_x/CZ, and WO_x/C catalysts..... 87

Fig. 4-8. NH_3-TPD profiles of WO_x/Z, WO_x/CZ, and WO_x/C catalysts..... 88

Fig. 4-9. CO_2-TPD profiles of WO_x/Z, WO_x/CZ, and WO_x/C catalysts..... 89

Fig. 4-10. Propylene conversion and propylene oxide selectivity with time on stream in the propylene

epoxidation by oxygen over WO_x/Z, WO_x/CZ, and WO_x/C catalysts at 400 ºC.....90

Chapter 1. Introduction

1.1. Propylene oxide (PO)

Propylene oxide (PO) with a molecular formula of C_3H_6O is a colorless and highly reactive material. Propylene oxide is widely used in the production of various materials such as polyurethane, polyester resin, and propylene glycol. Commercially, propylene oxide has been produced by the chlorohydrin process and the Halcon process (Fig. 1-1) [1-4]. However, all these processes have many drawbacks from environmental and economical viewpoints. The chlorohydrin process has shortcomings in a sense that it produces large amount of chlorinated by-product and waste salts. The Halcon process also has problem, which accompanies a stoichiometric amount of co-product (styrene and t-butylalcohol), and requires additional treatment steps to separate the propylene oxide and the co-product. Meanwhile, HPPO process, which produces propylene oxide using hydrogen peroxide (H_2O_2), has been developed to replace the commercial processes [5,6]. Because of the relatively high cost of hydrogen peroxide, however, this process has been restricted in industry. Therefore, the direct synthesis of propylene oxide from propylene and oxygen has attracted much attention as a cheap and green chemical process.

Process	Reactions	Issues
Chlorohydrin (Dow, Asahi Glass, Tokuyama) 43%	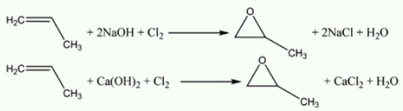	▪ High selectivity to PO (95%) ▪ Complex two-step system ▪ Requiring many extraction steps ▪ Environment problem
Propylene oxide / Styrene (PO/SM) (Lyondell, Shell) 33%	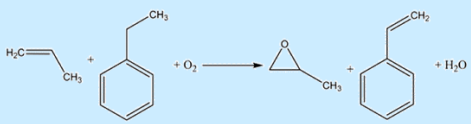	▪ High selectivity to PO (90%) ▪ Complex two-step system ▪ Formation of co-product (styrene)
Propylene oxide / Tert-butyl (PO/TBA) (Lyondell, Huntsman) 15%	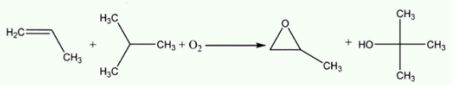	▪ High selectivity to PO (90%) ▪ Complex two-step system ▪ Formation of co-product (tert-butanol)
Hydrogen peroxide (HPPO) (DOW, BASF) 5%	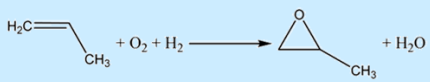	▪ High cost of reactant (H_2O_2)
Direct oxidation with O_2	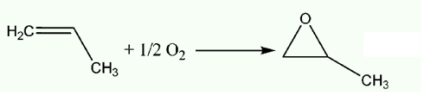	▪ Environment friendly ▪ Simple one-step system ▪ Low cost of reactant (O_2) ▪ Very low selectivity to PO (5%)

Fig. 1-1. Scheme for propylene oxide commercial production process.

1.2. Two reaction pathways for oxidation of propylene

There are two reaction pathways for the oxidation of propylene; complete oxidation and partial oxidation. Fig. 1-2 shows the two reaction pathways for oxidation of propylene. It has been reported that undesired complete oxidation ($C_3H_6 + 9/2O_2 \rightarrow 3CO_2 + 3H_2O$, $\Delta G = -1957.43$ kJ/mol) occur together with selective partial oxidation of propylene to propylene oxide ($C_3H_6 + 1/2O_2 \rightarrow 3C_3H_6O$, $\Delta G = -88.49$ kJ/mol) in the oxidation of propylene [7]. As shown in Fig. 1-2, propylene oxide is formed by the partial oxidation of propylene C=C π bond with molecular oxygen. On the other hand, H_2O and CO_2 are formed by the complete oxidation of allylic hydrogen C-H in propylene with molecular oxygen. For this reason, selectivity for propylene oxide in the direct epoxidation of propylene is thermodynamically limited. Therefore, many attempts have been made to improve the selectivity for propylene oxide in the direct epoxidation of propylene to propylene oxide.

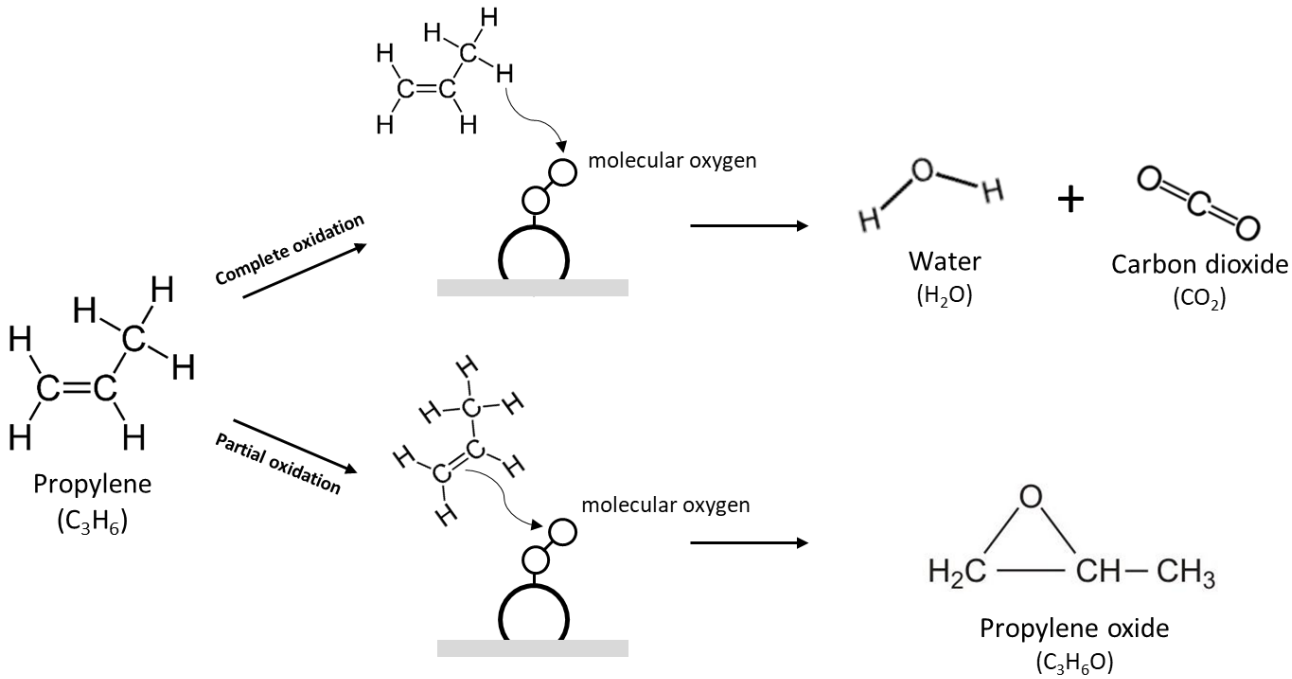

Fig. 1-2. Two reaction pathways for oxidation of propylene.

1.3. Difference between ethylene and propylene in the oxidation reaction

Fig. 1-3 shows the difference between ethylene and propylene in the oxidation reaction. It is well known that silver catalyst supported on α-alumina has found successful applications in the direct epoxidation of ethylene to ethylene oxide [8-10]. In the direct epoxidation of propylene to propylene oxide, however, silver catalyst supported on α-alumina showed a very low activity to propylene oxide. This is because the allylic C-H bond energy (77 kcal/mol) of propylene is lower than the vinylic C-H bond energy (112 kcal/mol) of ethylene [11]. For this reason, hydrogen abstraction of propylene, which is reaction of the allylic hydrogen and adsorbed oxygen to form H_2O and CO_2, is more favorable than that of ethylene. As a result, selectivity of propylene oxide over same catalyst applicated ethylene epoxidation is very low [9]. Therefore, many researches have been focused on developing an appropriate catalyst for the direct epoxidation of propylene to propylene oxide.

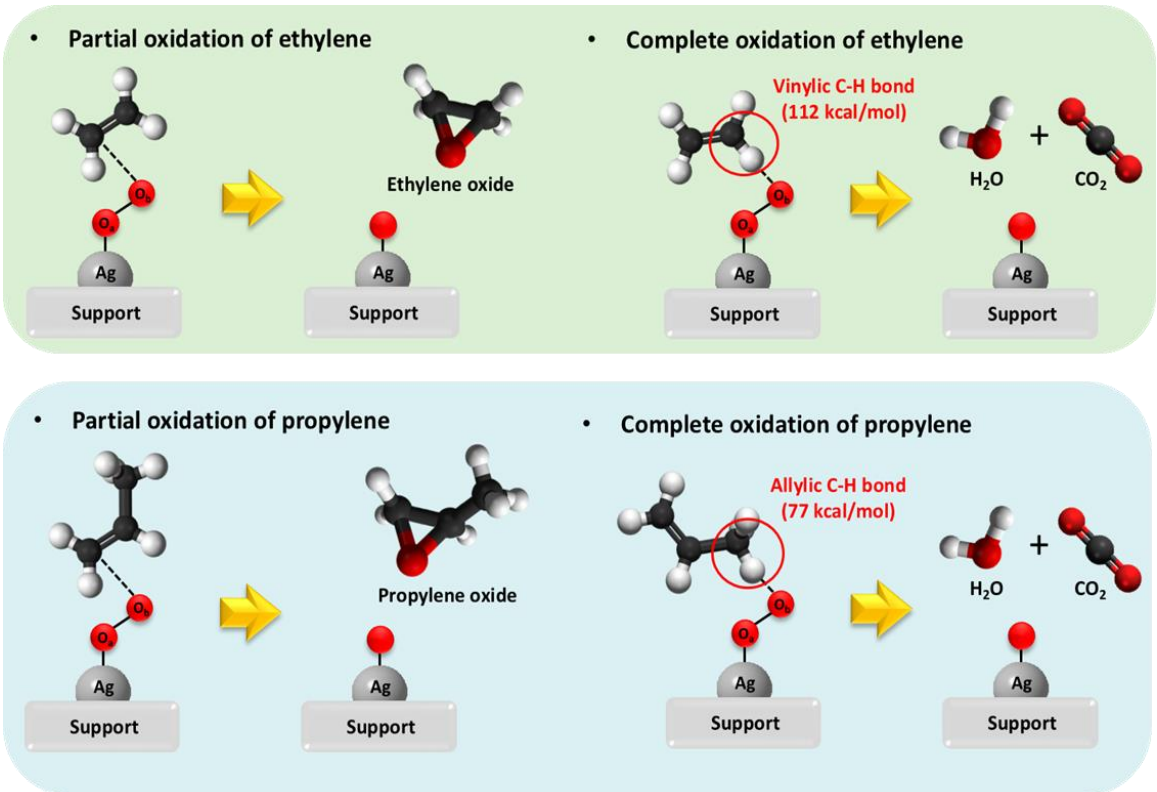

Fig. 1-3. Difference between ethylene and propylene in the oxidation reaction.

1.4. DAM (dipped adcluster model) theory

Fig. 1-4. shows the DAM theory mechanism. According to the DAM (dipped adcluster model) theory [12], electron in silver atom moves to adsorbed oxygen when oxygen is adsorbed on the silver active site. This indicates that adsorbed oxygen has a negative charge property, leading to reaction between adsorbed oxygen and allylic hydrogen. As a result, complete oxidation of propylene to H_2O and CO_2 occurs. When promotors such as alkali (earth) and transition metals are introduced to silver catalyst, however, negative charge property of oxygen adsorbed on silver site is reduced, resulting in inhibiting complete oxidation of propylene. It is well known that promotors such as alkali (earth) and transition metals decrease the negative charge property of oxygen adsorbed on the silver site, because promotors, which draw electrons from silver atom, reduce the flow of electrons from silver atom to adsorbed oxygen [13]. As a result, adsorbed oxygen has a relatively strong electrophilic property, resulting in a decrease of complete oxidation and resulting in an increase of reaction possibility between adsorbed oxygen and olefinic carbon. Therefore, electronic property of adsorbed oxygen played a key role in determining the catalytic performance of catalyst in the direct epoxidation of propylene to propylene oxide.

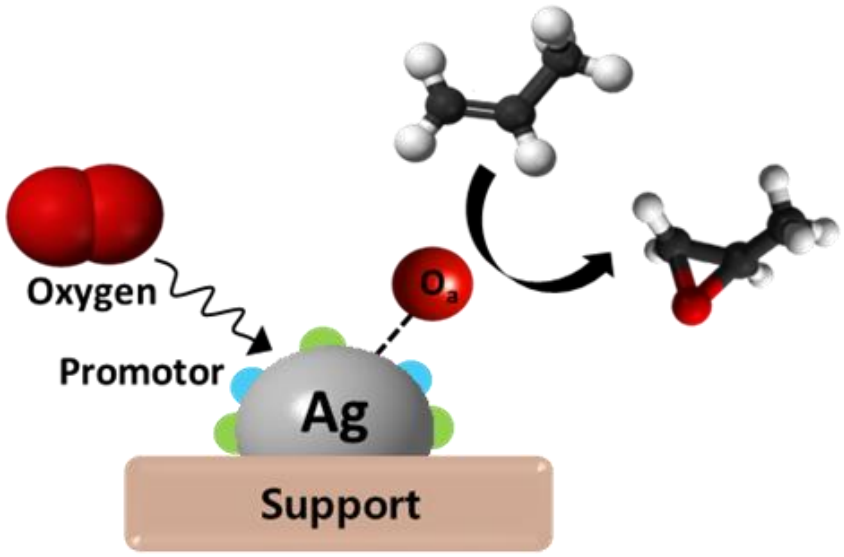

Fig. 1-4. DAM (dipped adcluster model) theory mechanism.

Chapter 2. Direct epoxidation of propylene to propylene oxide with molecular oxygen over Ag-(x)Mo-(5-x)W/ZrO_2 catalysts

2.1. Introduction

Propylene oxide (PO) is an important intermediate because it is used as a precursor for various chemicals such as polyester resin, propylene glycol, and polyurethane. Propylene oxide is commercially produced by Halcon process, chlorohydrin process, and HPPO (hydrogen peroxide-propylene oxide) process [1-6]. However, these processes involve many drawbacks in economical and environmental viewpoints. In order to overcome these problems, direct synthesis of propylene oxide from propylene and molecular oxygen has attracted much attention as a cheap and green chemical process.

Silver catalyst supported on α-alumina is well known to be the most efficient catalyst in the direct epoxidation of ethylene to ethylene oxide [8-10]. However, this catalyst shows a very low catalytic activity in the direct epoxidation of propylene to propylene oxide. It has been reported that allylic C-H bond energy (77 kcal/mol) in propylene is lower than vinylic C-H bond energy (112 kcal/mol) in ethylene [11]. This means that total oxidation of adsorbed molecular oxygen and C-H bond in propylene is more preferable than that in ethylene. As a consequence, H_2O and CO_2 rather than propylene oxide are mainly produced in the direct epoxidation of propylene.

Oxidation of propylene follows two reaction pathways; total oxidation and partial oxidation [14,15]. Total oxidation to H_2O and CO_2 occurs by the reaction of adsorbed molecular oxygen with allylic hydrogen (C-H) in propylene, whereas partial oxidation to propylene oxide occurs by the reaction of oxygen adsorbed on the silver active site with C=C π bond in propylene. This means that less nucleophilic property of adsorbed molecular oxygen is more favorable to enhance the reaction possibility between C=C π bond in propylene and adsorbed oxygen on the silver active site [14-16]. Therefore, modification of silver catalyst and change of electronic property of adsorbed oxygen can be a good strategy to enhance the selectivity for propylene oxide. In an attempt to improve the selectivity for propylene oxide in the direct epoxidation of propylene, introduction of various promotors such as alkali (earth), chlorine, and transition metals has been investigated [13,16-18].

In this work, a series of Ag-(x)Mo-(5-x)W/ZrO_2 catalysts were prepared by a slurry method with a variation of molybdenum content (x, wt%), and they were applied to the direct epoxidation of propylene to propylene oxide with molecular oxygen. The effect of molybdenum content on the physicochemical properties and catalytic activities was investigated.

2.2. Experimental

2.2.1. Preparation of catalysts

A series of Ag-(x)Mo-(5-x)W/ZrO_2 catalysts were prepared by a slurry method. Fig. 2-1 shows the preparation procedures for Ag-(x)Mo-(5-x)W/ZrO_2 catalysts. In short, 1.63 g of oxalic acid (C_2H2O_4, Junsei) and 0.9 ml of ethylene diamine ($C_2H_8N_2$, Sigma-Aldrich) were dissolved in distilled water (6 ml). After it was stirred for a few minutes, 1 g of silver oxide (Ag_2O, Sigma-Aldrich) was dissolved in the solution. Known amounts of ammonium molybdate ($(NH_4)_6Mo_7O_{24}\cdot 4H_2O$, Samchon) and ammonium (para) tungstate hydrate ($(NH_4)_{10}H_2(W_2O_7)_6\cdot xH_2O$, Sigma-Aldrich) were then added into the solution. After stirring the solution for 1 h, 3.54 g of zirconium oxide (ZrO_2, Sigma-Aldrich) was slowly added into the solution to form a slurry. After vigorous stirring the mixed slurry at 70 ^oC, it was evaporated to obtain a solid. The product was then dried at 120 ^oC in a convection oven for 1 day. The resultant was grinded and calcined at 460 ^oC for 3 h to obtain Ag-(x)Mo-(5-x)W/ZrO_2 catalysts. The prepared catalysts were denoted as Ag-(x)Mo-(5-x)W/ZrO_2 (x = 5, 3.75, 2.50, 1.25, and 0), where x represented wt% of molybdenum in the catalysts. Silver content in all the Ag-(x)Mo-(5-x)W/ZrO_2 catalysts was fixed at 20 wt%.

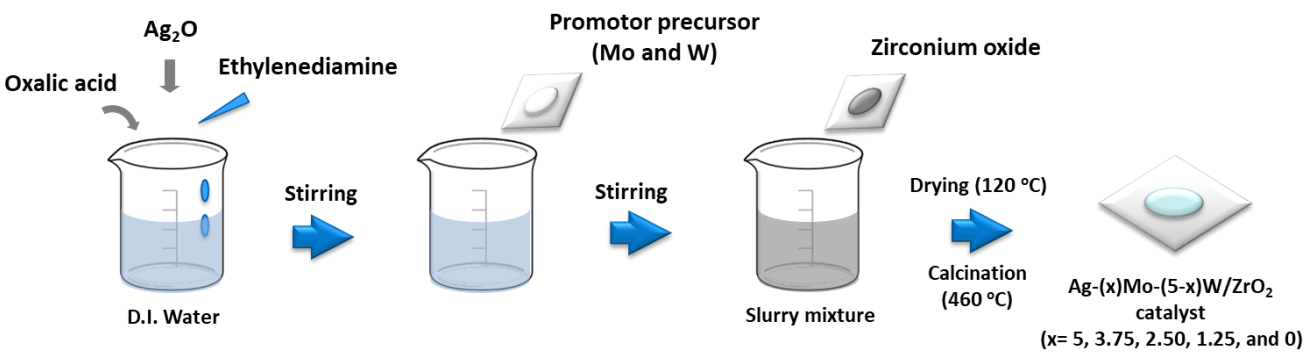

Fig. 2-1. Preparation procedure for Ag-(x)Mo-(5-x)W/ZrO_2 (x = 5, 3.75, 2.50, 1.25, and 0) catalysts.

2.2.2. Characterizations

N_2 adsorption-desorption measurements were carried out to examine the textural properties of Ag-(x)Mo-(5-x)W/ZrO_2 catalysts with a BELSORP-mini II (BEL Japan) instrument. Metal contents in the catalysts were determined by ICP-AES (Shimadz, ICP-1000IV) analyses. Crystalline structures of the catalysts were investigated by X-ray diffraction (XRD) measurements (D-Max2500-PC, Rigaku). Surface morphologies of the catalysts were examined by high resolution-transmission electron microscopy (HR-TEM) analysis (Jeol, JEM-3010). SEM analyses (Jeol, JSM-6700F) were conducted with energy dispersed X-ray spectroscopy (EDX) mapping to confirm the distribution of metal species. X-ray photoelectron spectroscopy (XPS) analyses (Sigma probe) were carried out to measure the binding energies of silver (Ag $3d_{5/2}$ and Ag $3d_{3/2}$) in the catalysts. All the XPS spectra were calibrated using C 1s peak (284.5 eV) as a reference.

2.2.3. Catalyst reaction tests

Direct epoxidation of propylene to propylene oxide with molecular oxygen was tested in a continuous flow fixed-bed quartz reactor at 460 ℃ under atmosphere pressure. Each catalyst (0.3 g) was thermally treated at 460 ℃ in a stream of nitrogen prior to the catalytic reaction. After treating the reactor with nitrogen for 30 min, propylene and oxygen were continuously supplied into the reactor with a nitrogen carrier. Feed composition was fixed at propylene:oxygen:nitrogen = 1.5:1:9. Total feed rate with respect to catalyst weight was maintained at 3000 ml/h · gcat. Reaction products were periodically sampled and analyzed with gas chromatographs (Younglin, ACME 6100) equipped with a thermal conductivity detector (Molsieve 5A and Porapak N columns) and a flame ionization detector (DB-1 column). Conversion of propylene and selectivity for propylene oxide were calculated on the bascs of carbon balance as follows.

$$\text{Conversion of propylene (\%)} = \frac{\text{mole of propylene reacted}}{\text{mole of propylene supplied}} \times 100$$

$$\text{Selectivity for propylene oxide (\%)} = \frac{\text{mole of propylene oxide formed}}{\text{mole of propylene reacted}} \times 100$$

2.3. Results and discussion

2.3.1. Characterization of Ag-(x)Mo-(5-x)W/ZrO_2 catalysts

Detailed textural properties of Ag-(x)Mo-(5-x)W/ZrO_2 (x = 5, 3.75, 2.50, 1.25, and 0) catalysts determined by N_2 adsorption-desorption measurements are listed in Table 2-1. All the catalysts exhibited very low surface area (< 10 m^2/g) and small pore volume (< 0.02 cm^3/g), indicating that they existed in the form of bulk-type catalysts. These textural properties are advantageous for propylene epoxidation, because well-developed porosity and high surface area are known to cause total oxidation of propylene [19]. Actual silver, molybdenum, and tungsten contents in the Ag-(x)Mo-(5-x)W/ZrO_2 catalysts were similar to the designed values.

Crystalline structures of Ag-(x)Mo-(5-x)W/ZrO_2 (x = 5, 3.75, 2.50, 1.25, and 0) catalysts were investigated by XRD measurements as shown in Fig. 2-2. All the catalysts showed four characteristic diffraction peaks (2θ= 38°, 44°, 64°, and 77°) which were ascribed to the crystal faces of silver (111), (200), (220), and (311). All the catalysts also showed diffraction peaks of tetragonal ZrO_2 (2θ= 34° and 49°) and monoclinic ZrO_2 (2θ= 28° and 31°), in good agreement with the previous result [20]. Diffraction peaks of molybdenum oxide and tungsten oxide were also observed at 2θ= 27° and 2θ= 29°, respectively. This means that Ag-(x)Mo-(5-x)W/ZrO_2 catalysts were successfully prepared as attempted in this work.

Surface morphologies and distributions of silver, molybdenum, tungsten,

and zirconium species in the Ag-(3.75)Mo-(1.25)W/ZrO_2 catalyst were confirmed by HR-TEM and SEM-EDX analyses as shown in Fig. 2-3. In the HR-TEM and SEM images (black and white), the catalyst existed in the form of bulk-type particles (100-300 nm). It is noticeable that silver atom (blue dot), molybdenum atom (purple dot), tungsten atom (red dot), and zirconium atom (yellow dot) were co-presented in the bulk particle domain of Ag-(3.75)Mo-(1.25)W/ZrO_2 catalyst. This result supports that silver, molybdenum, tungsten, and zirconium species were finely dispersed in the Ag-(3.75)Mo-(1.25)W/ZrO_2 catalyst.

Fig. 2-4 shows the SEM-EDX mapping images of reused Ag-(3.75)Mo-(1.25)W/ZrO_2 catalyst. Reused Ag-(3.75)Mo-(1.25)W/ZrO_2 catalyst showed no great difference in distribution of metal species compared to fresh Ag-(3.75)Mo-(1.25)W/ZrO_2 catalyst. In particular, no significant silver sintering was found after the reaction. Thus, Ag-(3.75)Mo-(1.25)W/ZrO_2 catalyst served as a stable catalyst in the direct epoxidation of propylene.

Electronic state of silver species in the Ag-(x)Mo-(5-x)W/ZrO_2 (x = 5, 3.75, 2.50, 1.25, and 0) catalysts was confirmed by XPS analyses as shown in Fig 2-5. For comparison, XPS analysis of Ag/ZrO_2 catalyst was also conducted (not shown in Fig. 4). All the Ag-(x)Mo-(5-x)W/ZrO_2 catalysts with molybdenum and/or tungsten promotor exhibited higher binding energies of Ag $3d_{5/2}$ and Ag $3d_{3/2}$ than Ag/ZrO_2 catalyst (368.1 eV (Ag $3d_{5/2}$) and 374.1 eV (Ag $3d_{3/2}$)). This result indicates that addition of promotor causes high binding energy of silver due to electron transfer from silver atom to promotor species. Binding energies of Ag $3d_{5/2}$ and Ag $3d_{3/2}$ were different with a variation of molybdenum content. Detailed binding energies of Ag $3d_{5/2}$ and

Ag $3d_{3/2}$ of the catalysts are summarized in Table 2-1. The binding energy of Ag 3d increased in the order of Ag-(5)W/ZrO_2 < Ag-(5)Mo/ZrO_2 < Ag-(1.25)Mo-(3.75)W/ZrO_2 < Ag-(2.50)Mo-(2.50)W/ZrO_2 < Ag-(3.75)Mo-(1.25)W/ZrO_2. Among the catalysts, Ag-(3.75)Mo-(1.25)W/ZrO_2 catalyst showed the highest binding energy shift of Ag 3d. When the transition metal materials are adjacent to each other, the valence states and the metal d-states are accompanied by large variations. It has been also reported that electron acceptor/donor property depend on the relative fraction of empty states in the valence band of the metal. Therefore, the d-state of each metal was changed by the introduction of the transition metal materials Mo and W, and it is considered that the electron acceptor property was influenced.

According to the dipped adcluster model (DAM) theory [12], movement of electron occurs from silver atom to adsorbed oxygen when molecular oxygen is adsorbed on the silver surface. This movement of electron leads to total oxidation reaction between allylic hydrogen in propylene and adsorbed oxygen due to negative charge property of adsorbed oxygen. When promotor, which draws electron from silver atom, is added into silver catalyst, however, nucleophilicity of molecular oxygen adsorbed on silver surface is reduced, leading to suppressed total oxidation of propylene. It has been reported that promotors such as transition and alkali (earth) metals alleviate the nucleophilicity of adsorbed oxygen [16-18]. This is because promotors lead to reduction of electron flow from silver atom to adsorbed oxygen. As a result, relatively strong electrophlicity of adsorbed oxygen inhibits total oxidation of adsorbed molecular oxygen with allylic hydrogen in propylene and increases reaction possibility between olefinic carbon and

adsorbed oxygen. Thus, it is expected that Ag-(3.75)Mo-(1.25)W/ZrO_2 catalyst would serve as an efficient catalyst in the direct epoxidation of propylene to propylene oxide.

2.3.2. Catalytic performance in the direct epoxidation of propylene to propylene oxide

Catalytic performance of Ag-(x)Mo-(5-x)W/ZrO_2 (x = 5, 3.75, 2.50, 1.25, and 0) catalysts in the direct epoxidation of propylene with molecular oxygen is shown in Fig. 2-6. It was found that all the Ag-(x)Mo-(5-x)W/ZrO_2 catalysts showed higher selectivity for propylene oxide than Ag/ZrO_2 catalyst (48.8 % conversion and 2.3 % selectivity) and they exhibited a stable catalytic performance during the whole reaction time. Ag-(x)Mo-(5-x)W/ZrO_2 (x = 5, 3.75, 2.50, 1.25, and 0) catalysts showed a considerable difference in selectivity for propylene oxide with respect to molybdenum content. Selectivity for propylene oxide increased in the order of Ag-(5)W/ZrO_2 < Ag-(5)Mo/ZrO_2 < Ag-(1.25)Mo-(3.75)W/ZrO_2 < Ag-(2.50)Mo-(2.50)W/ZrO_2 < Ag-(3.75)Mo-(1.25)W/ZrO_2. This trend was well consistent with the trend of binding energy shift of Ag 3d.

To investigate the reusability of the catalyst, reusability test for direct epoxidation of propylene over Ag-(3.75)Mo-(1.25)W/ZrO_2 catalyst was performed. Fig. 2-7 shows the reusability test result for direct epoxidation of propylene to propylene oxide over Ag-(3.75)Mo-(1.25)W/ZrO_2 catalyst. It was found that both fresh and reused catalysts showed similar catalytic performance. Thus, Ag-(3.75)Mo-(1.25)W/ZrO_2 catalyst served as a reusable catalyst in the direct epoxidation of propylene to propylene oxide.

Fig. 2-8 shows the correlation between binding energy shift of Ag $3d_{5/2}$ and selectivity for propylene oxide over Ag-(x)Mo-(5-x)W/ZrO_2 (x = 5, 3.75,

2.50, 1.25, and 0) catalysts. Binding energy shift of Ag $3d_{5/2}$ was calculated by the difference of binding energy of Ag $3d_{5/2}$ of the catalyst with respect to that of Ag-(5)W/ZrO_2. It should be noted that selectivity for propylene oxide increased with increasing binding energy shift of Ag $3d_{5/2}$. As mentioned earlier, high selectivity for propylene oxide in the direct epoxidation of propylene can be achieved by enhancing electrophilicity (reducing nucleophilicity) of adsorbed oxygen on the silver active site. This means that electron transfer from silver atom to adsorbed molecular oxygen should be suppressed for favorable catalytic performance. Thus, it is concluded the improved selectivity for propylene oxide over Ag-(x)Mo-(5-x)W/ZrO_2 catalysts was attributed to the binding energy shift of Ag 3d caused by the introduction of promotor.

Table 2-1. Physicochemical properties and XPS results of Ag-(x)Mo-(5-x)W/ZrO_2 (x = 5, 3.75, 2.50, 1.25, and 0) catalysts

Sample	Ag content (wt%)[a]	Mo content (wt%)[a]	W content (wt%)[a]	Surface area (m^2/g)[b]	Pore volume (cm^3/g)[c]	Binding energy (eV)	
						Ag $3d_{5/2}$	Ag $3d_{3/2}$
Ag-(5)Mo/ZrO_2	18.7	4.7	-	8.3	0.02	368.6	374.6
Ag-(3.75)Mo-(1.25)W/ZrO_2	19.5	3.61	1.37	6.0	0.02	369.2	375.3
Ag-(2.50)Mo-(2.50)W/ZrO_2	21.3	2.56	2.53	7.3	0.02	369.1	375.2
Ag-(1.25)Mo-(3.75)W/ZrO_2	20.4	1.23	3.42	7.0	0.02	368.9	375.0
Ag-(5)W/ZrO_2	19.4	-	5.1	6.7	0.02	368.4	374.3

[a] Determined by ICP-AES measurement
[b] Calculated by the BET (Brunauer–Emmett–Teller) equation
[c] Total pore volume at $P/P_0 = 0.99$

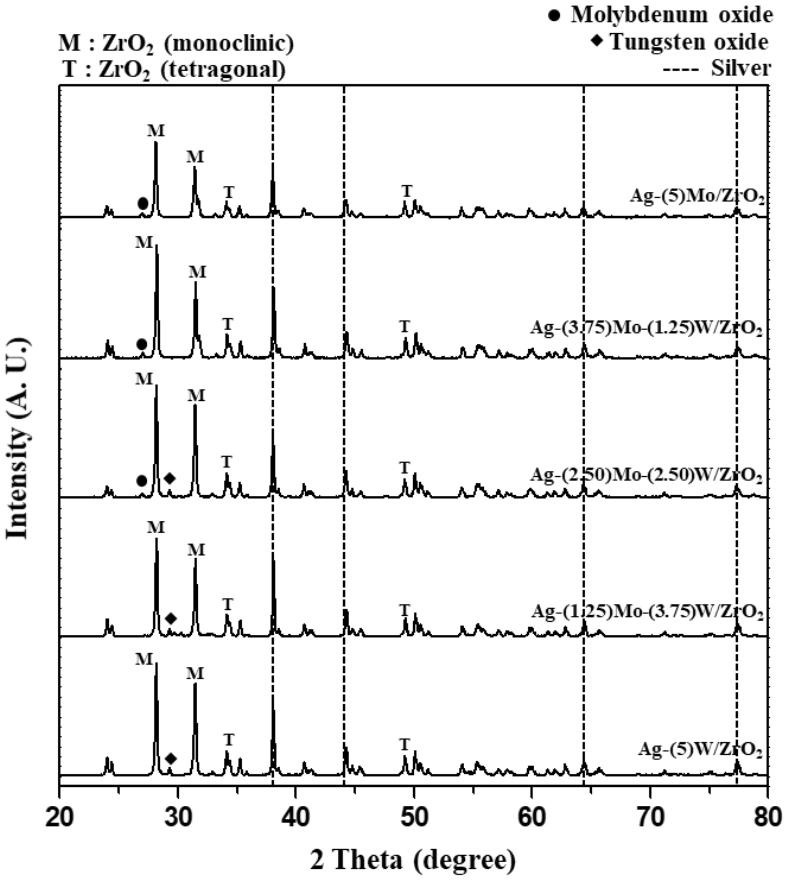

Fig. 2-2. XRD patterns of Ag-(x)Mo-(5-x)W/ZrO_2 (x = 5, 3.75, 2.50, 1.25, and 0) catalysts.

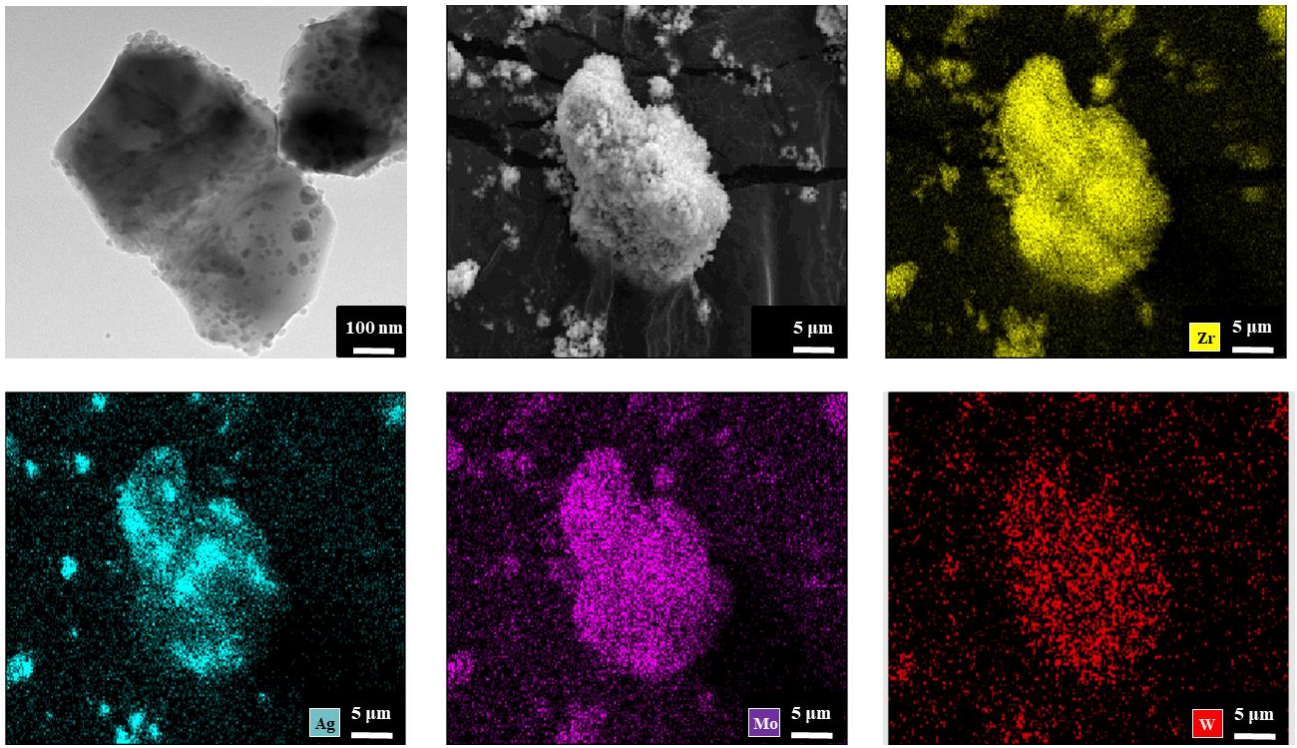

Fig. 2-3. HR-TEM and SEM-EDX mapping images of Ag-(3.75)Mo-(1.25)W/ZrO_2 catalyst.

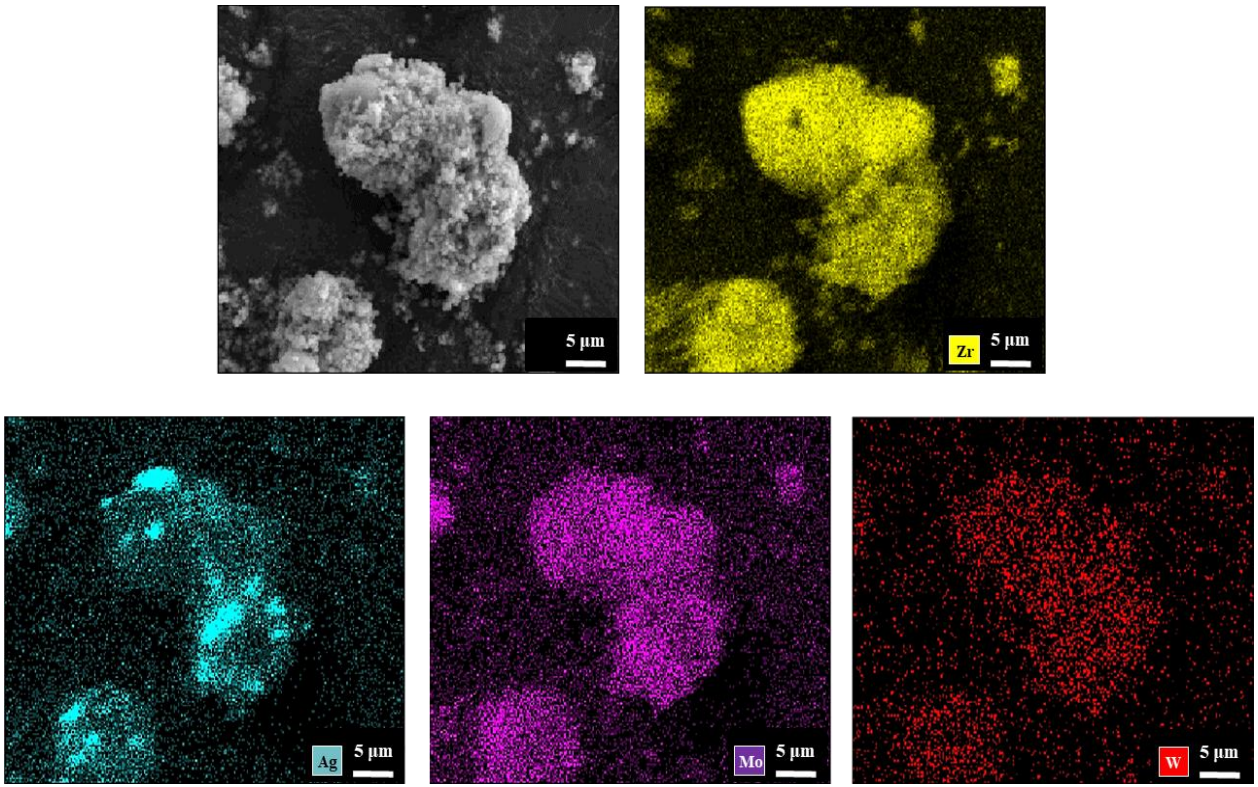

Fig. 2-4. SEM-EDX mapping images of reused Ag-(3.75)Mo-(1.25)W/ZrO_2 catalyst.

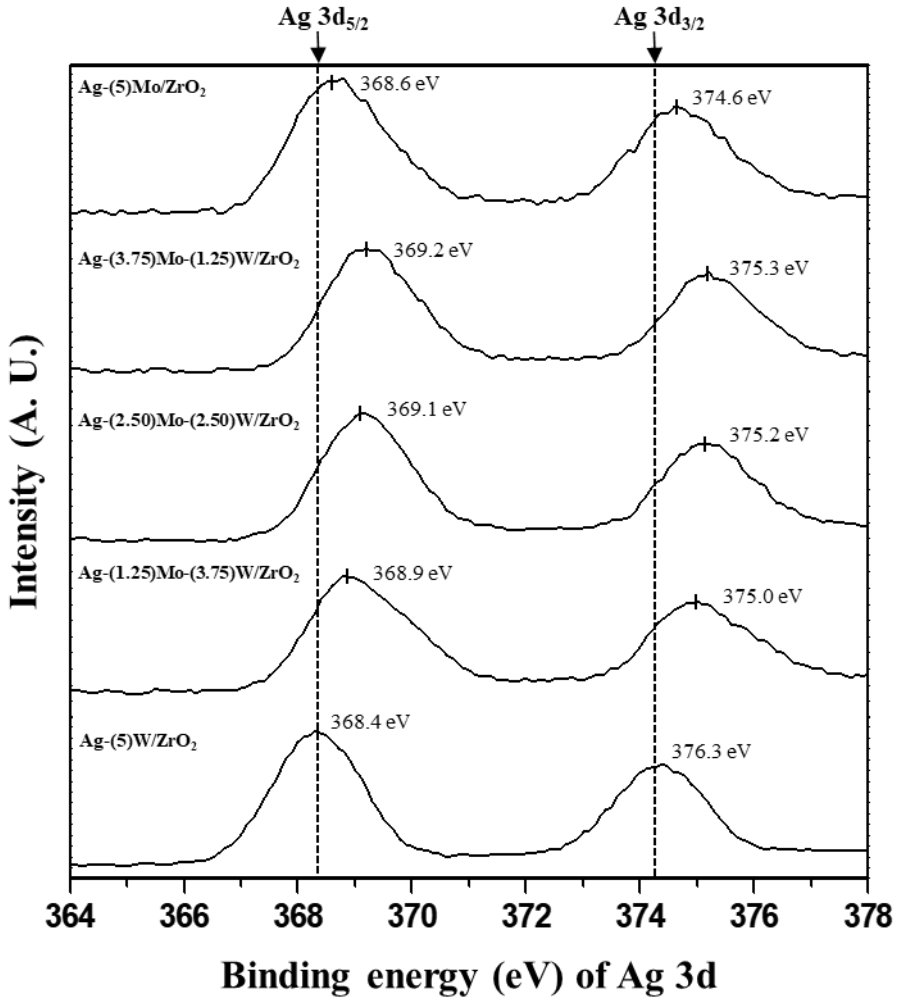

Fig. 2-5. XPS spectra of Ag $3d_{5/2}$ and Ag $3d_{3/2}$ of Ag-(x)Mo-(5-x)W/ZrO_2 (x = 5, 3.75, 2.50, 1.25, and 0) catalysts.

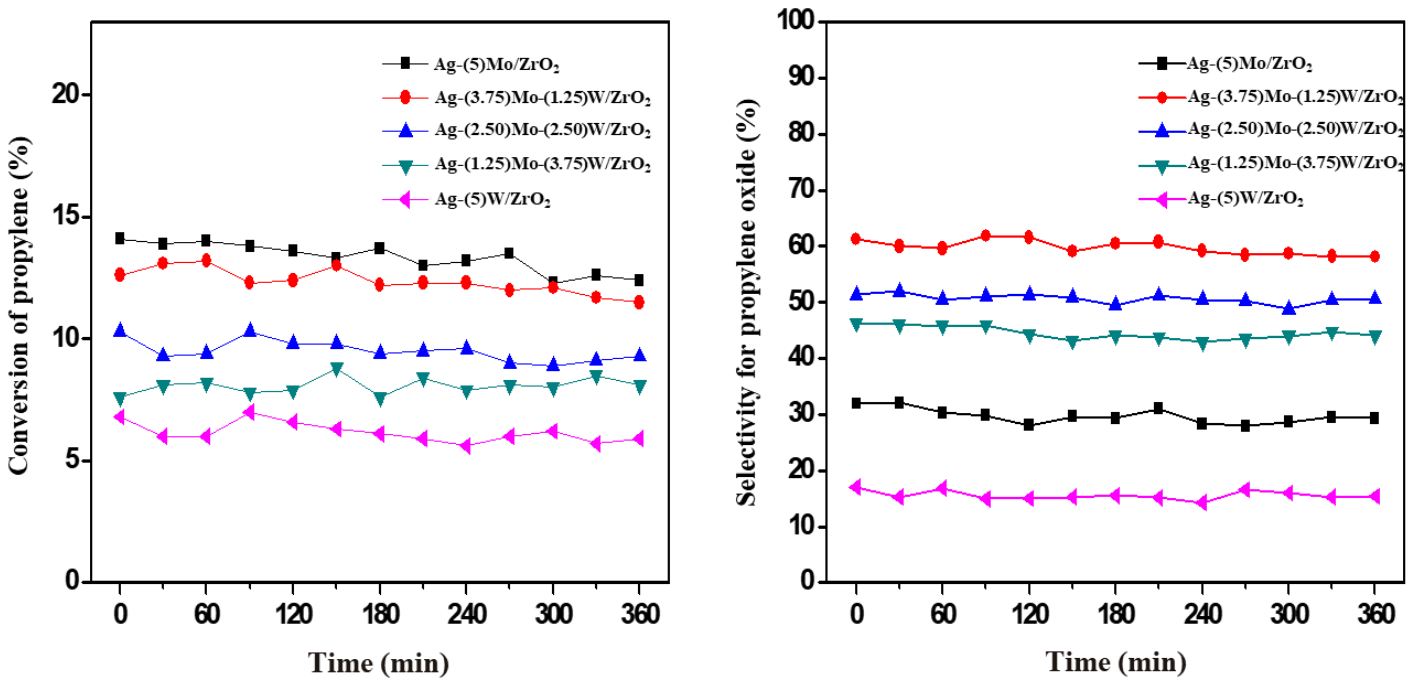

Fig. 2-6. Catalytic performance of Ag-(x)Mo-(5-x)W/ZrO_2 (x = 5, 3.75, 2.50, 1.25, and 0) catalysts with time on stream in the direct epoxidation of propylene to propylene oxide at 460 °C.

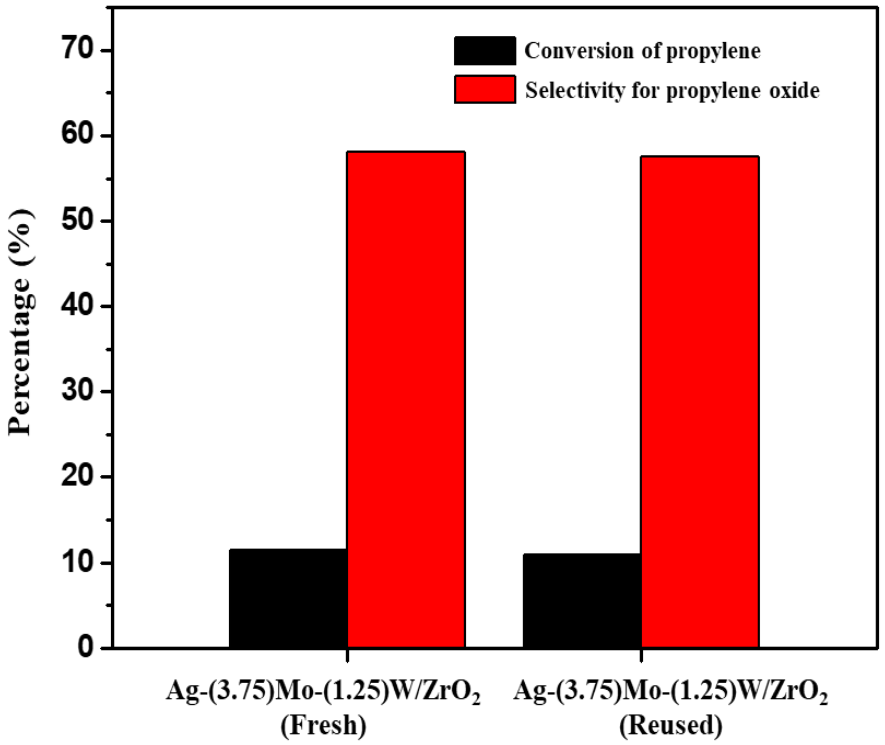

Fig. 2-7. Reusability test result for direct epoxidation of propylene to propylene oxide over Ag-(3.75)Mo-(1.25)W/ZrO_2 catalyst.

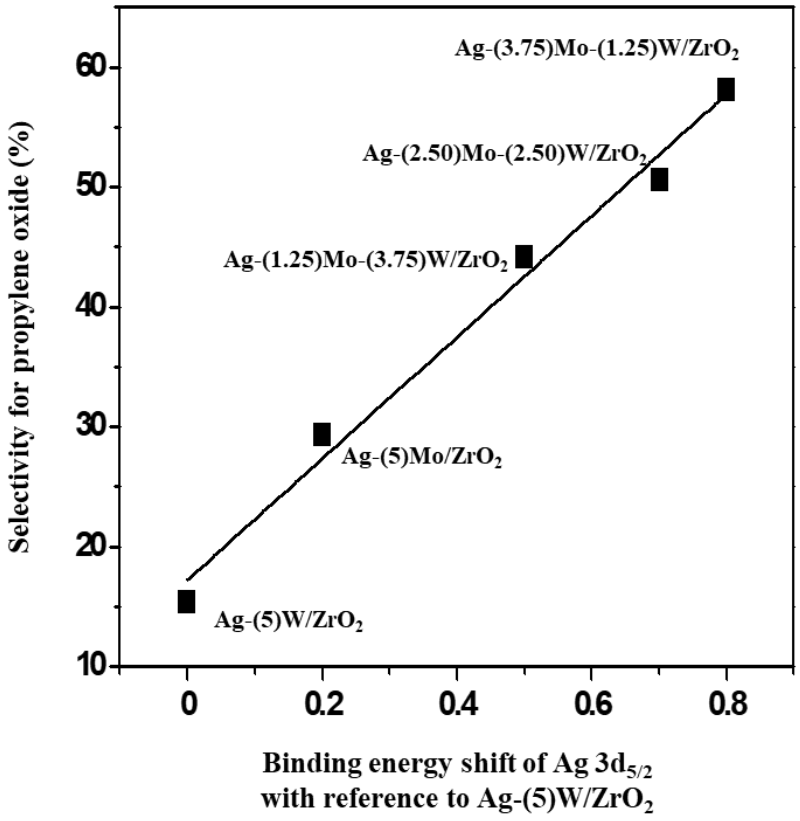

Fig. 2-8. A correlation between selectivity for propylene oxide and binding energy shift of Ag $3d_{5/2}$ of Ag-(x)Mo-(5-x)W/ZrO_2 (x = 5, 3.75, 2.50, 1.25, and 0) catalysts with reference to Ag-(5)W/ZrO_2.

Chapter 3. Direct epoxidation of propylene to propylene oxide over Ag-(Mo-W)/ZrO_2 catalysts: Effect of pH in the preparation of ZrO_2 support by a precipitation method

3.1. Introduction

Propylene oxide is a valuable material in petrochemical industries because it can be used as a precursor for important chemicals such as polyether polyol, propylene glycol, polyester resin, and polyurethane. Propylene oxide is currently produced from indirect process (Halcon process and Chlorohydrin process) and HPPO (hydrogen peroxide-propylene oxide) process [2,3,6,21,22]. Although high selectivity for propylene oxide over 90% is achieved with these processes, environmental issue and high price of hydrogen peroxide have been posed in the production of propylene oxide. In this respect, direct epoxidation of propylene to propylene oxide with molecular oxygen has attracted much attention as an efficient process that can replace the conventional processes.

For direct production of propylene oxide from propylene and oxygen, Ag/α-Al_2O_3 catalyst for producing ethylene oxide, which exhibits a similar

mechanism for propylene epoxidation, has been attempted [9,23,24]. However, $Ag/\alpha\text{-}Al_2O_3$ catalyst shows a very low selectivity for propylene oxide due to the difference in dissociation energy of C-H bond in propylene and ethylene. According to the literature [11,25], allylic C-H bond (77 kcal/mol) of propylene, which has lower dissociation energy than vinylic C-H bond (112 kcal/mol) of ethylene, causes a facile total oxidation of propylene to H_2O and CO_2, leading to low selectivity for propylene oxide over $Ag/\alpha\text{-}Al_2O_3$ catalyst. Therefore, development of an appropriate catalyst system is needed for the direct epoxidation of propylene.

In an attempt to develop an efficient catalyst, direct epoxidation of propylene has been investigated over a number of catalysts based on silver metal supported on various materials such as alkali-earth metal oxide [19,26-28], $\alpha\text{-}Al_2O_3$ [29], and ZrO_2 [18,30]. It has been reported that production of propylene oxide through propylene epoxidation is influenced by physicochemical properties of supporting materials such as crystalline phase or acid/base property [11,31]. ZrO_2 is known to exhibit the characteristic physicochemical properties as a supporting material [32,33]. According to the literatures [34,35], the physicochemical properties of ZrO_2 can be controlled by changing ZrO_2 preparation method. Thus, it is expected that selectivity for propylene oxide in the direct epoxidation of propylene can be modulated by changing ZrO_2 preparation method. Therefore, a systematic investigation on the effect of ZrO_2 preparation method on the physicochemical properties and

catalytic activities of Ag-based catalysts supported on ZrO_2 would be worthwhile.

In this work, a series of ZrO_2 (pH X) supports were prepared by a precipitation method with a variation of pH (X) of ZrO_2 solution, and subsequently, Ag-(Mo-W)/ZrO_2 (pH X) catalysts were prepared by a slurry method for use in the direct epoxidation of propylene to propylene oxide with molecular oxygen. The effect of pH condition for preparing ZrO_2 on the physicochemical propertiy and catalytic activities of Ag-(Mo-W)/ZrO_2 (pH X) catalysts was investigated. The prepared catalysts were characterized by N_2 adsorption-desorption, ICP-AES, XRD, FE-SEM, SEM-EDX, NH_3-TPD, and CO_2-TPD analyses.

3.2. Experimental

3.2.1. Preparation of catalysts

A series of ZrO_2 supports were prepared by a precipitation method with a variation of pH (3, 6, 10, 12, and 14) value of ZrO_2 solution according to the procedures reported in the literature [36]. Fig. 3-1 shows the preparation procedures for ZrO_2 (pH X) (X = 3, 6, 10, 12, and 14) supports. 9.25 g of zirconium oxynitrate hydrate ($ZrO(NO_3)_2 \cdot xH_2O$, Sigma-Aldrich) was dissolved in 200 ml of distilled water. After it was stirred for 15 min, ammonium hydroxide solution (NH_4OH, Sigma–Aldrich) was added dropwise into the zirconium precursor solution at a constant rate (5 ml/min). The pH (3, 6, 10, 12, and 14) of the solution was controlled by changing the amount of ammonium hydroxide solution. After the resulting solution was stirred vigorously at room temperature for 6 h, it was aged overnight at room temperature. The precipitate was filtered and washed with distilled water and ethanol successively. The precipitate was then separated by centrifuge, and it was dried overnight at 100 ^oC. The dried product was finally calcined at 600 ^oC for 6 h to yield ZrO_2 support. The prepared ZrO_2 support was denoted as ZrO_2 (pH X) (X = 3, 6, 10, 12, and 14), where X represented the pH value of ZrO_2 solution for precipitation.

For the preparation of Ag-(Mo-W)/ZrO_2 (pH X) catalysts, silver and

promotors (Mo and W) were introduced onto ZrO_2 (pH X) support by a slurry method [37]. Fig. 3.1 shows the preparation procedures Ag-(Mo-W)/ZrO_2 (pH X) (X = 3, 6, 10, 12, and 14) catalysts. In short, 0.5 ml of ethylene diamine ($C_2H_8N_2$, Sigma-Aldrich) and 0.55 g of oxalic acid ($C_2H_2O_4$, Junsei) were simultaneously dissolved in distilled water (6 ml). 0.34 g of silver oxide (Ag_2O, Sigma-Aldrich) was then dissolved in the solution. Ag content in the catalysts was fixed at 20 wt%. After stirring the mixture for 1 h, 0.02 g of ammonium (para) tungstate hydrate ($(NH_4)_{10}H_2(W_2O_7)_6 \cdot xH_2O$, Sigma-Aldrich) and 0.058 g of ammonium molybdate ($(NH_4)_6Mo_7O_{24} \cdot {}_4H_2O$, Sigma-Aldrich) were additionally dissolved in the solution. Mo content and W content in the catalysts were fixed at 3.75 wt% and 1.25 wt%, respectively. After stirring the resulting solution, 1.2 g of ZrO_2 (pH X) was slowly added into the solution to form a slurry. After the mixed slurry was stirred vigorously at 70 ^oC for 4 h, it was evaporated to obtain a solid. After grinding the dried solid, it was finally calcined at 460 ^oC for 3 h with an air stream to yield Ag-(Mo-W)/ZrO_2 (pH X) (X = 3, 6, 10, 12, and 14) catalysts.

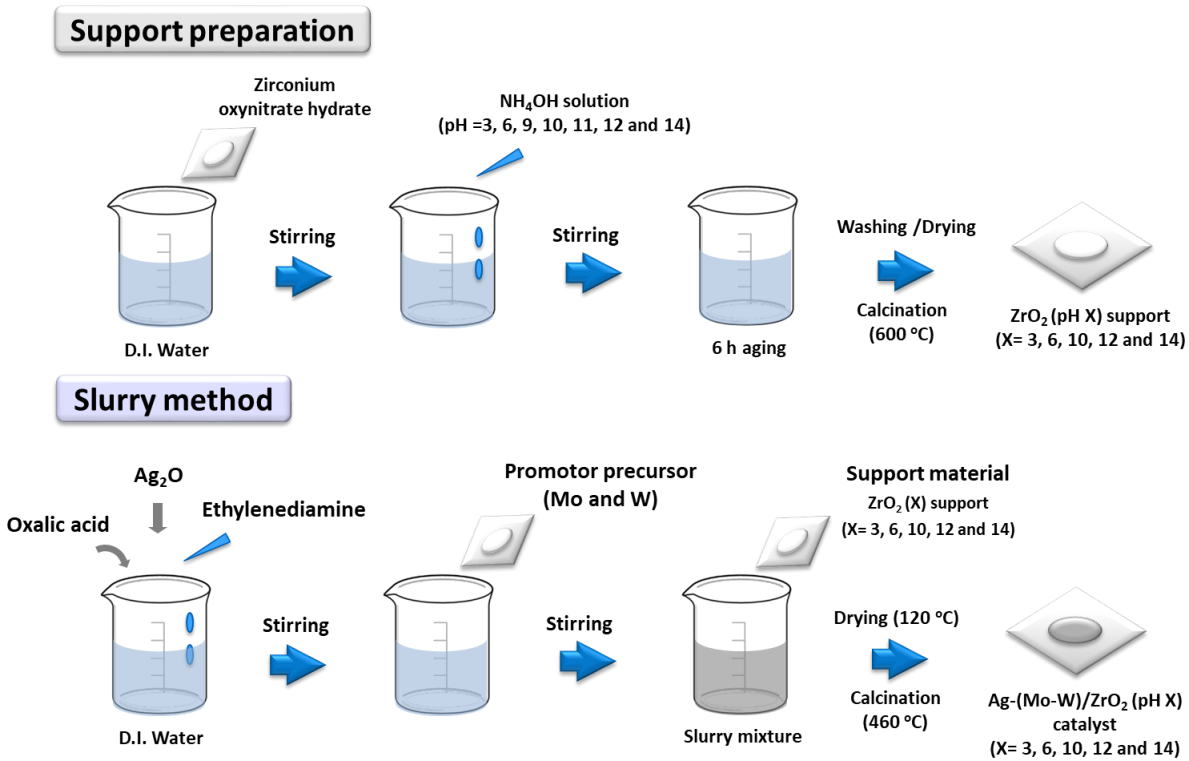

Fig. 3-1. Preparation procedure for ZrO_2 (pH X) (X = 3, 6, 10, 12, and 14) supports and Ag-(x)Mo-(5-x)W/ZrO_2 (x = 5, 3.75, 2.50, 1.25, and 0) catalysts.

3.2.2. Characterizations

Chemical compositions of Ag-(Mo-W)/ZrO_2 (pH X) catalysts were determined by ICP-AES (Shimadz, ICP-1000IV) analyses. Textural properties of Ag-(Mo-W)/ZrO_2 (pH X) catalysts were measured by N_2 adsorption-desorption measurements (BELSORP-mini II, BEL Japan). Before the analyses, all the catalysts were degassed using a rotary vacuum pump at 150 ^oC for 3 h to remove impurities and moisture. Surface areas of the catalysts were determined by the BET (Brunaur-Emmett-Teller) method at relative pressure (P/P_0) of 0.05-0.30. Pore volumes of the catalysts were determined by the BJH (Barrett-Joyner-Halenda) method applied to the desorption branch of the N_2 isotherm. Crystalline phases of ZrO_2 (pH X) supports and Ag-(Mo-W)/ZrO_2 (pH X) catalysts were investigated by XRD measurements (Rigaku, D-MAX2500-PC) using Cu-Ka radiation (λ = 1.54056 A˚) operated at 50 kV and 100 mA. Surface morphologies of the catalysts were examined by FE-SEM (Scanning Electron Microscope) analyses (JSM-6700F, Jeol). To confirm the distribution of metal species of the catalysts, energy dispersive X-ray spectroscopy (EDX) mapping analyses were conducted (JSM-6700F, Jeol). Acidity of the catalysts was measured by NH_3-TPD (temperature-programmed desorption) experiments (BEL Japan, BELCAT-B). In order to remove any physisorbed organic molecules, 0.05 g of each catalyst was treated in the TPD apparatus at 200 ^oC for 2 h with a stream of helium (50 ml/min). After cooling the catalyst to 25 ^oC, NH_3 (50 ml) gas was injected into the reactor in a stream of helium (30 ml/min) to saturate acid sites of the catalyst. Physisorbed

ammonia was removed at 100 ^{o}C for 1 h under a flow of helium (50 ml/min). After cooling the catalyst, NH_3-TPD measurement was conducted within the temperature range of 50–500 ^{o}C under a helium flow (50 ml/min). Thermal conductivity detector (TCD) was used for the detection of desorbed NH_3. Basicity of the catalysts was measured by CO_2-TPD experiments. Experimental procedures for CO_2-TPD were identical to those for NH_3-TPD, except that CO_2 instead of NH_3 was used as a probe molecule.

3.2.3. Catalytic reaction tests

Production of propylene oxide by direct epoxidation of propylene with molecular oxygen was conducted in a continuous flow fixed-bed quartz reactor under atmosphere pressure. Feed composition was fixed at propylene:oxygen:nitrogen = 1.5:1:9. Total feed rate with respect to catalyst weight was maintained at 7004 ml/h · g. Catalytic reaction was carried out at 460 °C. Reaction products were periodically sampled and analyzed with gas chromatographs (Younglin, ACME 6100) equipped with a thermal conductivity detector (Molsieve 5A and Porapak N columns) and a flame ionization detector (DB-1 column). Conversion of propylene and selectivity for propylene oxide were calculated on the basis of carbon balance as follows.

$$\text{Conversion of propylene (\%)} = \frac{\text{mole of propylene reacted}}{\text{mole of propylene supplied}} \times 100$$

$$\text{Selectivity for propylene oxide (\%)} = \frac{\text{mole of propylene oxide formed}}{\text{mole of propylene reacted}} \times 100$$

3.3. Results and discussion

3.3.1. Textural property and morphology of Ag-(Mo-W)/ZrO_2 (pH X) catalysts

Textural properties of Ag-(Mo-W)/ZrO_2 (pH X) (X = 3, 6, 10, 12, and 14) catalysts are summarized in Table 3-1. BET surface area and pore volume of Ag-(Mo-W)/ZrO_2 (pH X) catalysts showed no significant difference with respect to pH value. All the catalysts showed very low surface area (< 10 m^2/g) and small pore volume (< 0.02 cm^3/g). This result indicates that all the Ag-(Mo-W)/ZrO_2 (pH X) catalysts were successfully prepared as bulk-type catalysts. According to the literature [31], high surface area and well-developed porous structure of the catalyst have a negative effect on the production of propylene oxide, because propylene oxide diffused into well-developed porous structure of the catalyst is deeply oxidized to H_2O and CO_2, resulting in the decrease of selectivity for propylene oxide. Silver and promotor metal contents in the Ag-(Mo-W)/ZrO_2 (pH X) catalysts determined by ICP-AES analyses were in good agreement with designed values. This means that all the Ag-(Mo-W)/ZrO_2 (pH X) catalysts were successfully prepared as attempted in this work.

Fig. 3-2 shows the FE-SEM images of Ag-(Mo-W)/ZrO_2 (pH X) (X = 3, 10, and 14) catalysts. The images of the catalysts clearly show that uniform

and bulk-type particles with a diameter of ca. 300 nm were successfully formed. In particular, all the catalysts showed the large pores due to its low porosity. As mentioned earlier, large pore with poor porous structure is beneficial to produce propylene oxide.

In order to confirm the homogeneous distribution of constituent elements, SEM-EDX mapping analyses were carried out. Fig. 3-3 shows the SEM-EDX mapping images of Ag-(Mo-W)/ZrO_2 (pH 10) catalyst. The elemental mapping images obtained for silver atom (blue dot), molybdenum atom (purple dot), tungsten atom (red dot), and zirconium atom (yellow dot) were matched with the SEM image (black and white). The EDX images of Ag-(Mo-W)/ZrO_2 (pH 10) catalyst clearly showed that all the metal species were uniformly distributed in the Ag-(Mo-W)/ZrO_2 (pH 10) catalyst.

Crystalline structures of ZrO_2 (pH X) supports and Ag-(Mo-W)/ZrO_2 (pH X) catalysts were confirmed by X-ray diffraction (XRD) measurements. Fig. 3-4 shows the XRD patterns of ZrO_2 (pH X) (X = 3, 6, 10, 12, and 14) supports. It was observed that all the ZrO_2 (pH X) supports exhibited the characteristic XRD peaks of monoclinic ZrO_2 ($2\theta = 28^o$ and 31^o) and tetragonal ZrO_2 ($2\theta = 30^o$) [38,39]. Interestingly, ZrO_2 (pH X) supports exhibited a significant difference in crystal structure of ZrO_2 with a variation of pH of ZrO_2 solution. This result was well consistent with the result of previous work [34], indicating that a series of ZrO_2 (pH X) supports with different crystal structure were successfully prepared in this work.

Fig. 3-5 shows the XRD patterns of Ag-(Mo-W)/ZrO_2 (pH X) (X = 3, 6, 10, 12, and 14) catalysts. All the catalysts exhibited several diffraction peaks (2θ= 38°, 44°, 64°, and 77°), which were attributed to the crystal faces of silver (111), (200), (220), and (311), respectively [40]. It is noted that the fraction of monoclinic phase in the Ag-(Mo-W)/ZrO_2 (pH X) catalysts was still maintained even after the introduction of silver and promotor (Mo and W).

The fraction of monoclinic phase of Ag-(Mo-W)/ZrO_2 (pH X) (X = 3, 6, 10, 12, and 14) catalysts calculated from XRD peaks (Fig. 3-4 and Fig. 3-5) is listed in Table 3-2. We used the ratio of XRD peak height ($(111)_M$ / $(101)_T$ + $(111)_M$) in order to measure the fraction of monoclinic phase in the ZrO_2 (pH X) supports [34]. The fraction of monoclinic phase in the catalysts decreased in the order of Ag-(Mo-W)/ZrO_2 (pH 10) > Ag-(Mo-W)/ZrO_2 (pH 12) > Ag-(Mo-W)/ZrO_2 (pH 6) > Ag-(Mo-W)/ZrO_2 (pH 3) > Ag-(Mo-W)/ZrO_2 (pH 14). This is because ZrO_2 phase (monoclinic or tetragonal) was modulated by controlling the pH value of ZrO_2 solution during the precipitation process [34,35]. It is known that monoclinic ZrO_2 phase serves as an efficient and active phase in the direct epoxidation of propylene compared to tetragonal ZrO_2 phase [31]. This implies that an appropriate pH condition of ZrO_2 solution is required to improve the catalytic performance.

3.3.2. NH_3-TPD and CO_2-TPD analyses of Ag-(Mo-W)/ZrO_2 (pH X) catalysts

In order to investigate the acid property of Ag-(Mo-W)/ZrO_2 (pH X) catalysts, NH_3-TPD experiment was carried out. Fig 3-6 shows the NH_3-TPD profiles of Ag-(Mo-W)/ZrO_2 (pH X) (X = 3, 6, 10, 12, and 14) catalysts. All the catalysts showed a broad NH_3-TPD peak at 150-300 ^oC. Acidity of the catalysts measured from NH_3-TPD peak area is summarized in Table 3-3. Acidity of Ag-(Mo-W)/ZrO_2 (pH X) catalysts was in the range of 0.16–0.61 mmol-NH_3/g. Acidity of Ag-(Mo-W)/ZrO_2 (pH X) catalysts decreased with increasing pH value of ZrO_2 solution.

CO_2-TPD experiment was conducted to determine the basicity of Ag-(Mo-W)/ZrO_2 (pH X) (X = 3, 6, 10, 12, and 14) catalysts as presented in Fig. 3-7. Basicity of the catalysts calculated from CO_2-TPD peak area is also listed in Table 3-3. Basicity of Ag-(Mo-W)/ZrO_2 (pH X) catalysts was in the range of 0.20–0.60 mmol-CO_2/g. Basicity of Ag-(Mo-W)/ZrO_2 (pH X) catalysts also decreased with increasing pH value of ZrO_2 solution.

Many researchers agree that the direct epoxidation of propylene to propylene oxide follows the DAM (dipped adcluster model) theory. According to this theory [12,41], there are two reaction pathways for oxidation of propylene; partial oxidation to form propylene oxide and complete oxidation to form H_2O and CO_2. It is known that acid site, which changes electronic

property of adsorbed oxygen less nucleophilic by accepting electrons from adsorbed oxygen, helps partial oxidation between oxygen adsorbed on silver and C=C π bond in propylene. On the other hand, basic site, which causes acid-base reaction between oxygen adsorbed on silver and basic site, leads to complete oxidation. That is, acid property plays a positive role in the production of propylene oxide, whereas base property gives a negative effect. To elucidate the effect of acidity and basicity on the catalytic performance of Ag-(Mo-W)/ZrO_2 (pH X) catalysts, we calculated the ratio of acidity with respect to basicity. The calculated ratio of acidity/basicity is listed in Table 3. The ratio of acidity/basicity decreased in the order of Ag-(Mo-W)/ZrO_2 (pH 10) > Ag-(Mo-W)/ZrO_2 (pH 12) > Ag-(Mo-W)/ZrO_2 (pH 6) > Ag-(Mo-W)/ZrO_2 (pH 3) > Ag-(Mo-W)/ ZrO_2 (pH 14), in good agreement with the trend of fraction of monoclinic phase of ZrO_2 (Table 2). Therefore, it can be inferred that the catalyst with high ratio of acidity/basicity would be favorable for the production of propylene oxide.

3.3.3. Catalytic performance in the direct epoxidation of propylene to propylene oxide

Fig. 3-8 shows the propylene conversion and propylene oxide selectivity with time on stream in the direct epoxidation of propylene over Ag-(Mo-W)/ZrO_2 (pH X) (X = 3, 6, 10, 12, and 14) catalysts at 460 ºC. Ag-(Mo-W)/ZrO_2 (pH X) catalysts showed a stable catalytic performance without any significant catalyst deactivation during the reaction. It was observed that propylene conversion of Ag-(Mo-W)/ZrO_2 (pH X) catalysts showed small variation (< 6 %) with respect to pH value of ZrO_2 solution. However, selectivity for propylene oxide of the catalysts strongly depended on pH value (X = 3, 6, 10, 12, and 14) of ZrO_2 solution. Selectivity for propylene oxide decreased in the order of Ag-(Mo-W)/ZrO_2 (pH 10) > Ag-(Mo-W)/ZrO_2 (pH 12) > Ag-(Mo-W)/ZrO_2 (pH 6) > Ag-(Mo-W)/ZrO_2 (pH 3) > Ag-(Mo-W)/ZrO_2 (pH 14). This trend was in good agreement with the trend of fraction of monoclinic phase (Table 3-2) and ratio of acidity/basicity (Table 3-3). Among the catalysts tested, Ag-(Mo-W)/ZrO_2 (pH 10) catalyst showed the highest catalytic performance in terms of selectivity for propylene oxide.

3.3.4. Correlations between catalytic performance and catalytic property

Fig. 3-9 shows the correlations between selectivity for propylene oxide and fraction of monoclinic phase, and between selectivity for propylene oxide and ratio of acidity/basicity of the catalysts. Selectivity for propylene oxide was well correlated with the fraction of monoclinic phase and the ratio of acidity/basicity. Selectivity for propylene oxide increased with increasing the fraction of monoclinic phase. As mentioned earlier, monoclinic ZrO_2 phase has been recognized as the most active phase for the direct epoxidation of propylene among the ZrO_2 phases. This correlation clearly demonstrates that high fraction of monoclinic phase of the catalyst was favorable for the production of propylene oxide from propylene and molecular oxygen. In addition, selectivity for propylene oxide increased with increasing the ratio of acidity/basicity of the catalysts. It is clear that high ratio of acidity/basicity of Ag-(Mo-W)/ZrO_2 (pH X) catalysts was also favorable for selective production of propylene oxide. Among the catalysts tested, Ag-(Mo-W)/ZrO_2 (pH 10) catalyst, which retained the highest fraction of monoclinic phase and the highest ratio of acidity/basicity, showed the best catalytic performance in the direct epoxidation of propylene to propylene oxide. Therefore, it is concluded that ZrO_2 crystalline phase and acid/base property of the catalysts played key roles in determining the catalytic performance of Ag-(Mo-W)/ZrO_2 (pH X) catalysts in the direct epoxidation of propylene to propylene oxide.

Table 3-1. Textural properties of Ag-(Mo-W)/ZrO_2 (pH X) (X = 3, 6, 10, 12, and 14) catalysts

Catalyst	Ag content (wt%)[a]	Mo content (wt%)[a]	W content (wt%)[a]	Surface area (m^2/g)[b]	Pore volume (cm^3/g)[c]
Ag-(Mo-W)/ZrO_2 (pH 3)	21.1	3.86	1.19	12.4	0.03
Ag-(Mo-W)/ZrO_2 (pH 6)	19.4	3.71	1.17	11.2	0.02
Ag-(Mo-W)/ZrO_2 (pH 10)	20.2	3.74	1.28	12.1	0.02
Ag-(Mo-W)/ZrO_2 (pH 12)	20.7	3.79	1.18	11.3	0.02
Ag-(Mo-W)/ZrO_2 (pH 14)	19.6	3.69	1.24	12.9	0.03

[a] Determined by ICP-AES measurement
[b] Calculated by the BET (Brunauer–Emmett–Teller) equation
[c] Total pore volume at $P/P_0 = 0.99$

Table 3-2. Fraction of monoclinic phase of Ag-(Mo-W)/ZrO_2 (pH X) (X = 3, 6, 10, 12, and 14) catalysts

Catalyst	Fraction of monoclinic phase[a]
Ag-(Mo-W)/ZrO_2 (pH 3)	0.38
Ag-(Mo-W)/ZrO_2 (pH 6)	0.59
Ag-(Mo-W)/ZrO_2 (pH 10)	0.91
Ag-(Mo-W)/ZrO_2 (pH 12)	0.79
Ag-(Mo-W)/ZrO_2 (pH 14)	0.19

[a] The ratio of XRD peak height ($(111)_M$ / $(101)_T$ + $(111)_M$) was used to estimate the fraction of monoclinic phase of zirconia (M: monoclinic phase / T: tetragonal phase)

Table 3-3. Acidity, basicity, and ratio of acidity/basicity of Ag-(Mo-W)/ZrO_2 (pH X) (X = 3, 6, 10, 12, and 14) catalysts

Catalyst	Acidity (mmol NH_3/g_{cat})[a]	Basicity (mmol CO_2/g_{cat})[b]	Acidity/basicity ratio
Ag-(Mo-W)/ZrO_2 (pH 3)	0.61	0.60	1.02
Ag-(Mo-W)/ZrO_2 (pH 6)	0.58	0.44	1.32
Ag-(Mo-W)/ZrO_2 (pH 10)	0.55	0.24	2.29
Ag-(Mo-W)/ZrO_2 (pH 12)	0.35	0.21	1.67
Ag-(Mo-W)/ZrO_2 (pH 14)	0.16	0.20	0.80

[a] Determined by NH_3-TPD measurement
[b] Determined by CO_2-TPD measurement

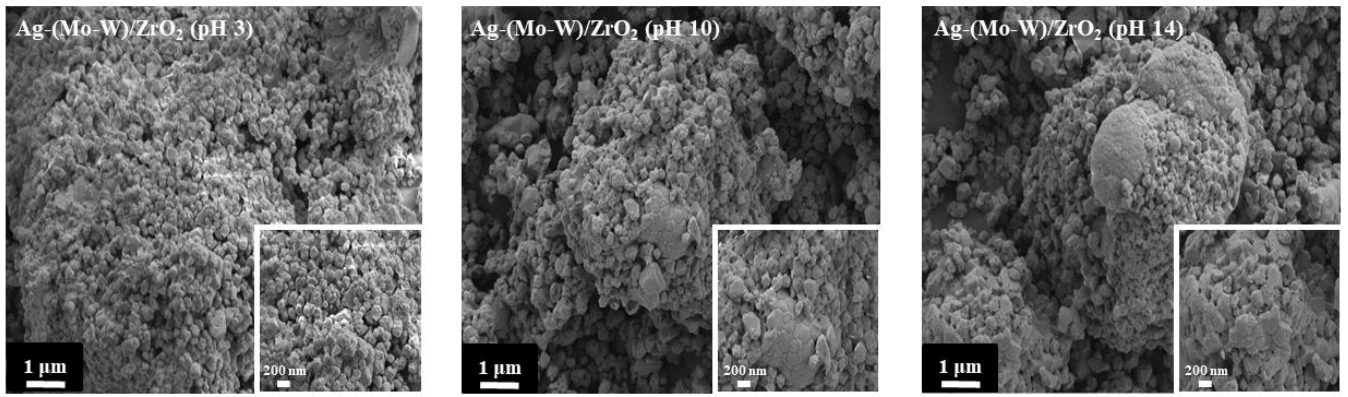

Fig. 3-2. FE-SEM images of Ag-(Mo-W)/ZrO_2 (pH X) (X = 3, 10, and 14) catalysts.

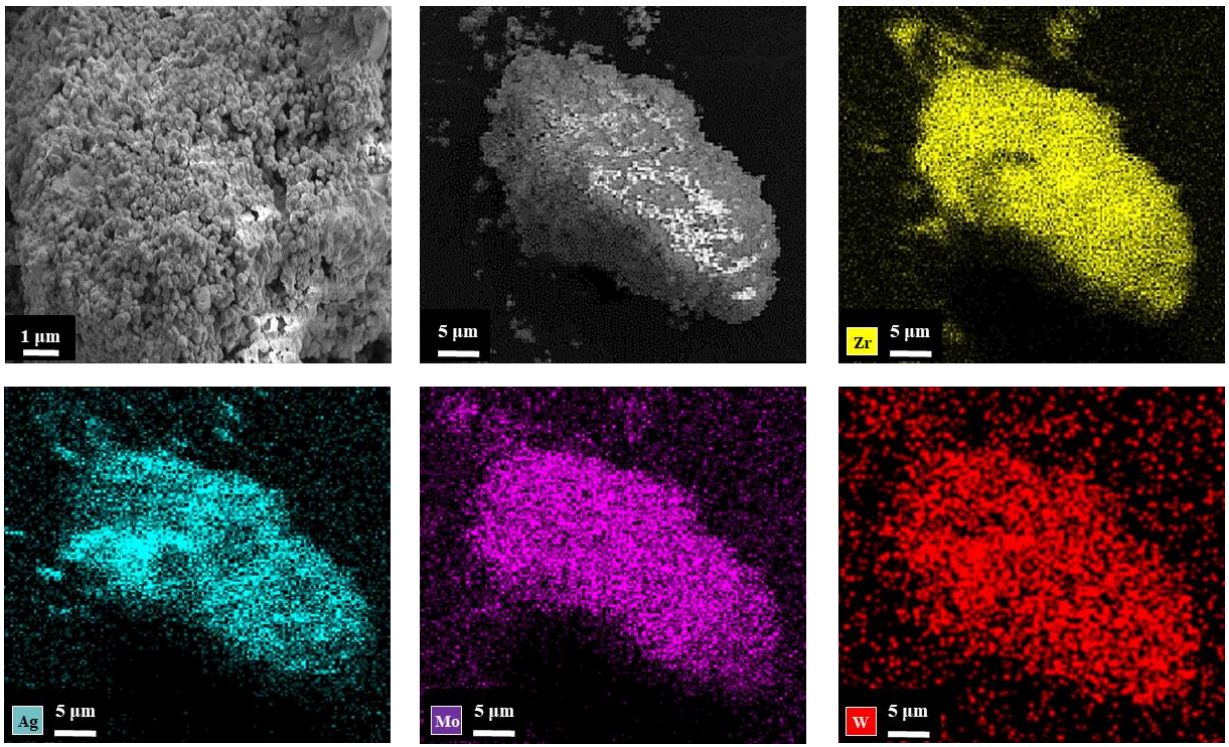

Fig. 3-3. SEM-EDX mapping images of Ag-(Mo-W)/ZrO_2 (pH 10) catalyst.

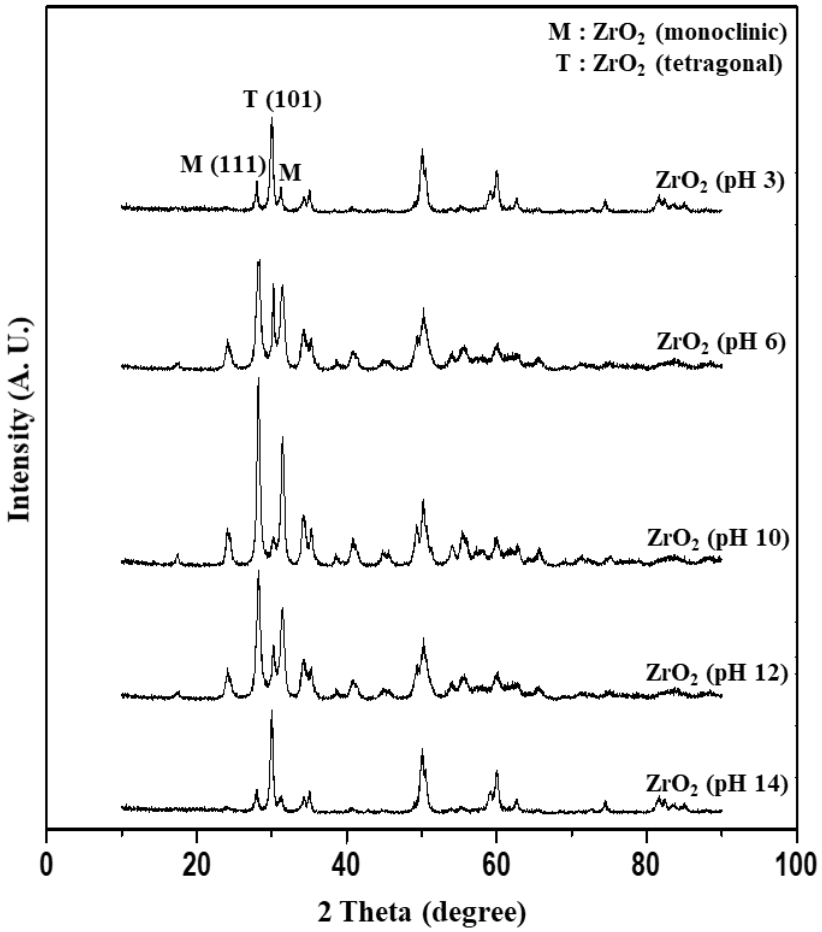

Fig. 3-4. XRD patterns of ZrO_2 (pH X) (X = 3, 6, 10, 12, and 14) supports.

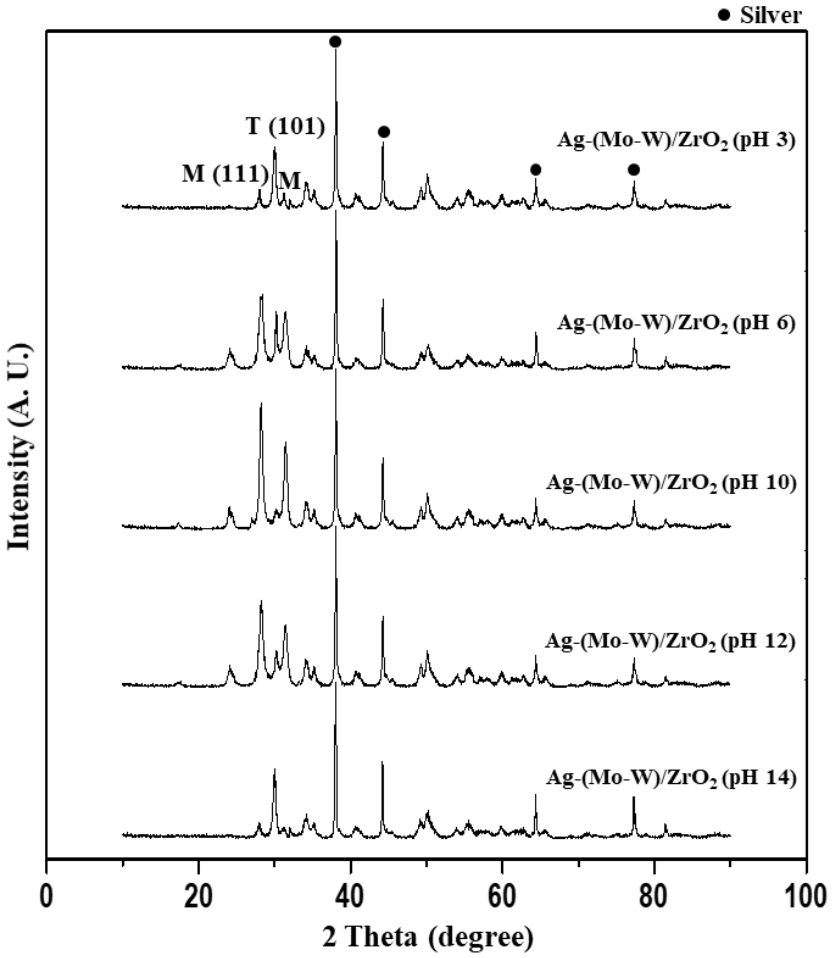

Fig. 3-5. XRD patterns of Ag-(Mo-W)/ZrO_2 (pH X) (X = 3, 6, 10, 12, and 14) catalysts.

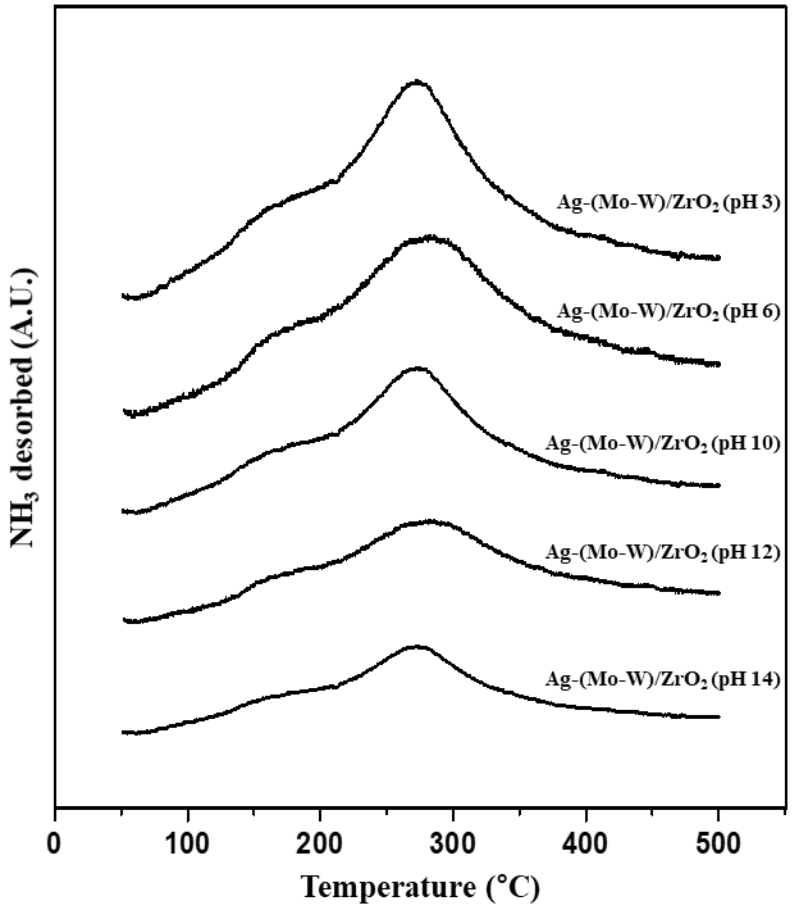

Fig. 3-6. NH_3-TPD profiles of Ag-(Mo-W)/ZrO_2 (pH X) (X = 3, 6, 10, 12, and 14) catalysts.

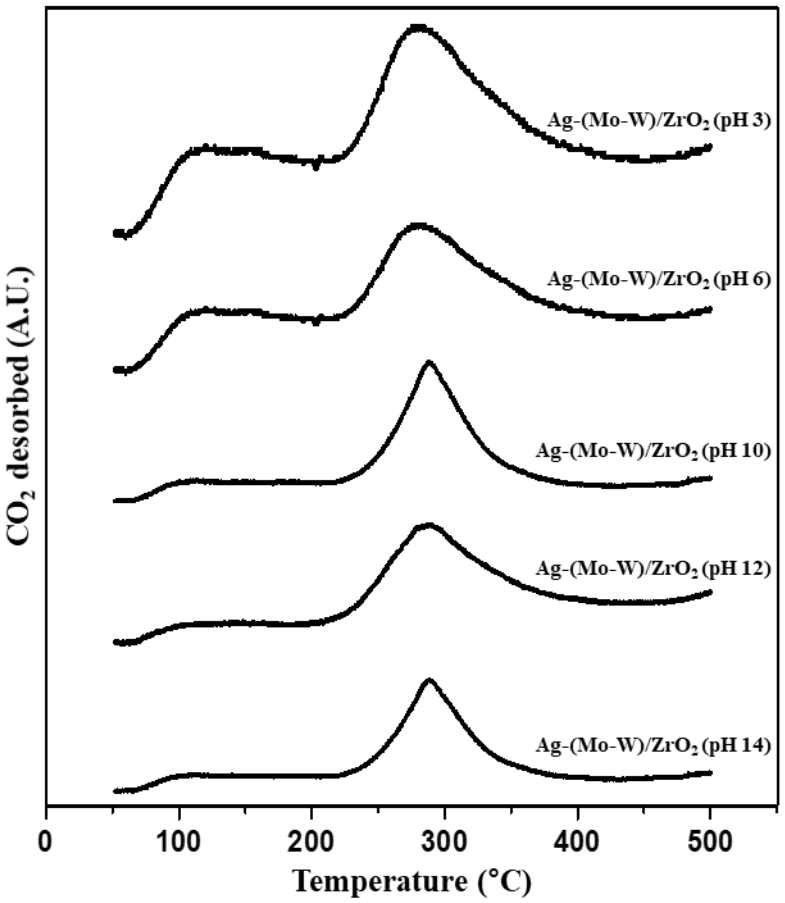

Fig. 3-7. CO_2-TPD profiles of Ag-(Mo-W)/ZrO_2 (pH X) (X = 3, 6, 10, 12, and 14) catalysts.

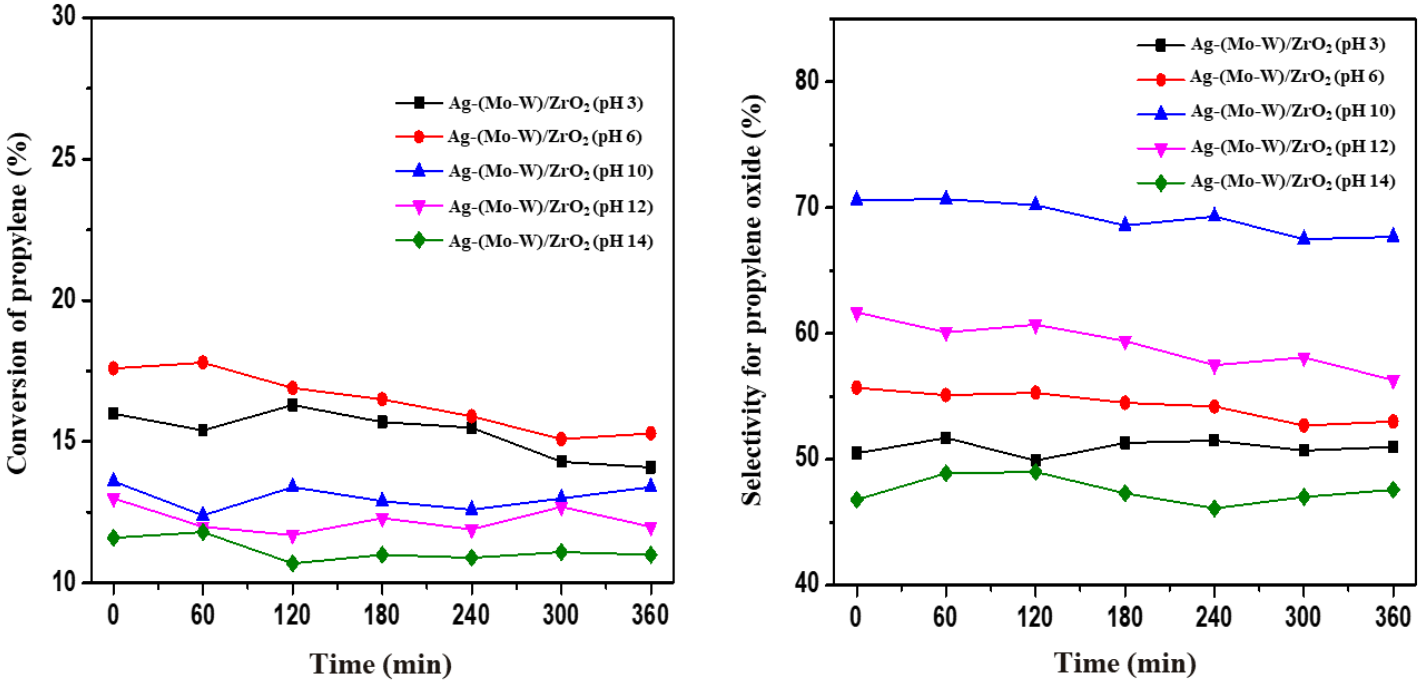

Fig. 3-8. Propylene conversion and propylene oxide selectivity with time on stream in the direct epoxidation of propylene over Ag-(Mo-W)/ZrO_2 (pH X) (X = 3, 6, 10, 12, and 14) catalysts at 460 ºC.

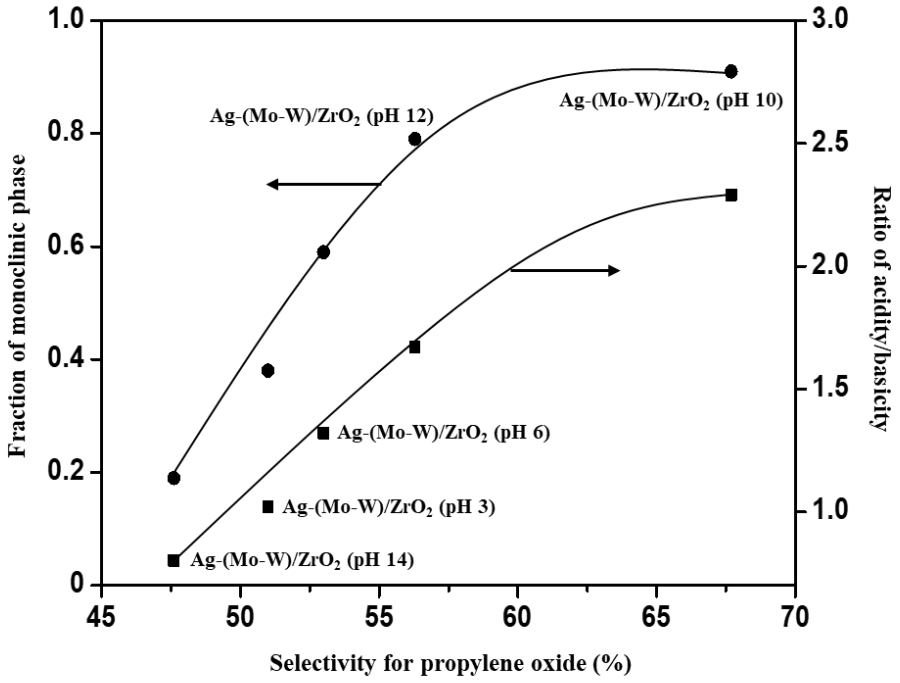

Fig. 3-9. Correlations between selectivity for propylene oxide and fraction of monoclinic phase, and between selectivity for propylene oxide and ratio of acidity/basicity of the catalysts.

Chapter 4. Propylene epoxidation by oxygen over tungsten oxide supported on ceria-zirconia

4.1. Introduction

Propylene oxide is crucial raw chemical for manufacturing various petrochemical products such as propylene glycol, polyurethane, polyether polyol, and polyester resin. Traditionally, propylene oxide is produced though indirect processes such as chlorohydrin process and Halcon process [1-3]. However, such processes have drawbacks in producing by-products such as styrene, tert-butyl alcohol, and chlorinated materials. In order to overcome these drawbacks, HPPO (hydrogen peroxide-propylene oxide) process has been developed to produce propylene oxide, but this process has a problem of supplying expensive hydrogen peroxide [6,42]. Therefore, propylene epoxidation by oxygen has received much attention as an attractive process for producing propylene oxide.

For propylene epoxidation by oxygen, Ag/α-Al_2O_3 catalyst, which is active for ethylene epoxidation has been attempted [9,24,43]. However, Ag/α-Al_2O_3 catalyst shows a very low selectivity for propylene oxide due to the difference in dissociation energy of C-H bond in propylene and ethylene. According to the literature [11,25], allylic C-H bond (77 kcal/mol) of

propylene, which has lower dissociation energy than vinylic C-H bond (112 kcal/mol) of ethylene, gives rise to the facile total oxidation of propylene to H_2O and CO_2, leading to low selectivity for propylene oxide over Ag/α-Al_2O_3 catalyst. Therefore, development of an appropriate catalyst system is needed for high propylene oxide production.

In an attempt to develop an efficient catalyst, selective epoxidation of propylene has been investigated over Ag-based catalyst system [18,19,27,28,44-46]. However, it is known that commercial Ag-based catalysts suffer from deactivation in the oxidation reaction, because silver particles are sintered during the oxidation reaction [47,48]. For these reasons, many researches have been focused on the metal oxide catalyst system in the propylene epoxidation by oxygen. Miller et al. reported that the propylene conversion of 1.0 % and selectivity for propylene oxide of 55-60 % were obtained over the SnO_2-CuO-NaCl/SiO_2 catalyst system [49]. Garcia-Aguilar et al. also prepared K-(Fe-Si)O_2 catalyst, over which 1.4 % propylene conversion and 65.5 % selectivity for propylene oxide were achieved in the gas-phase epoxidation of propylene [50]. WO_x/ZrO_2 catalyst has attracted attention due to their excellent thermal stability and significant redox property [51-53]. For example, WO_x/ZrO_2 showed high activity in the DBT (dibenzothiophene) oxidation due to the oxygen on the tungsten oxide surface [53]. However, any researches on the propylene epoxidation by oxygen over WO_x/ZrO_2 catalyst have not been reported yet. Also, it is well known that

CeO_2 has been widely employed as efficient catalysts for various catalytic reactions due to its oxygen storage/release ability [25,26]. Therefore, a systematic investigation of tungsten oxide catalyst supported on zirconia support containing ceria with excellent oxidation ability for the propylene epoxidation would be meaningful.

In this work, ZrO_2, $Ce_{0.05}Zr_{0.95}O_2$, and CeO_2 supports were prepared by a precipitation method, and subsequently, WO_x/Z, WO_x/CZ, and WO_x/C catalysts were prepared by a wetness impregnation method. WO_x/Z, WO_x/CZ, and WO_x/C catalysts were characterized by XRF, nitrogen adsorption–desorption, FE-SEM, SEM-EDX, XRD, H_2-TPR, NH_3-TPD, and CO_2-TPD analyses. Propylene epoxidation by oxygen was carried out over WO_x/Z, WO_x/CZ, and WO_x/C catalysts in a continuous flow reactor, and their catalytic activities were compared.

4.2. Experimental

4.2.1. Preparation of catalysts

The $CeZrO_2$ support was prepared by using a co-precipitation method (Fig. 4-1). Known amounts of cerium precursor ($Ce(NO_3)_3 \cdot 6H_2O$, 5 mol%) and zirconium precursor ($ZrO(NO_3)_2 \cdot xH_2O$, 95 mol%) were dissolved in distilled water. After dissolving all the precursors, ammonium hydroxide solution (NH_4OH, Sigma–Aldrich) was added dropwise into the cerium-zirconium precursor solution till the pH value of solution reached ca. 8. The solution was vigorously stirred at 25 °C for 6 h. This precipitate was washed with ethanol and distilled water to remove the residual organic materials. Then support powder was dried at 110 °C for 24 h and calcined at 500 °C for 3 h in an air stream to yield $CeZrO_2$ support. The prepared $CeZrO_2$ support was denoted as CZ. For comparison, ZrO_2 and CeO_2 supports were also prepared by using the same method described above and denoted as Z and C, respectively.

The $WO_x/CeZrO_2$ catalysts were prepared by using an impregnation method (Fig. 4-1). An appropriate amount of ammonium (para) tungstate hydrate ($(NH_4)_{10}H_2(W_2O_7)_6 \cdot xH_2O$, Sigma-Aldrich) was solved in distilled water (20 ml). The prepared $CeZrO_2$ support was then introduced into the solution under vigorous stirring, and the mixture was stirred at 60 ℃ for 6 h.

The resulting solid was dried at 110 ^{o}C for 24 h. The dried product was calcined for 3 h to yield $WO_x/CeZrO_2$ catalyst. The prepared $WO_x/CeZrO_2$ catalyst was denoted as WO_x/CZ. For comparison, WO_x/ZrO_2 and WO_x/CeO_2 catalysts were also prepared by using the same method described above and denoted as WO_x/Z and WO_x/C, respectively.

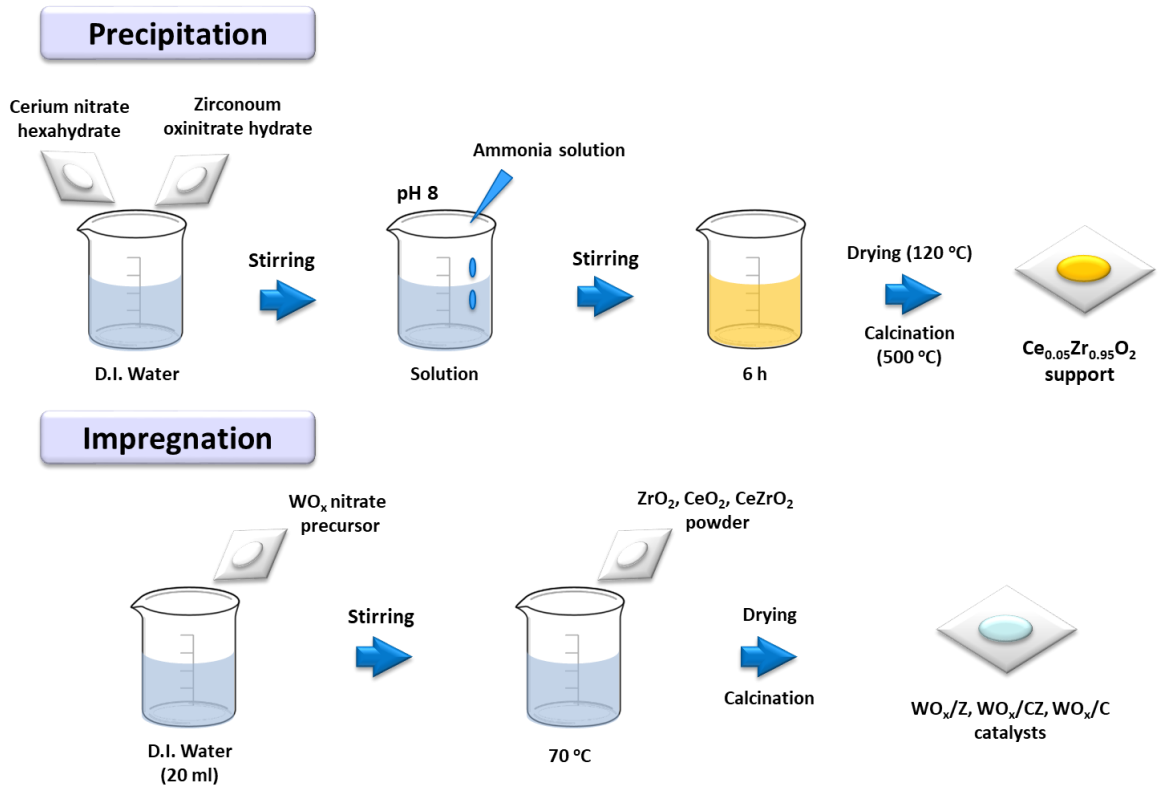

Fig. 4-1. Preparation procedure for ZrO_2, $CeZrO_2$, and CeO_2 supports and WO_x/ZrO_2, $WO_x/CeZrO_2$, and WO_x/CeO_2 catalysts.

4.2.2. Characterizations

WO_x contents and Zr/Ce ratios of each catalyst were determined by X-ray fluorescence (XRF) analysis. Surface areas and average pore diameter of WO_x/Z, WO_x/CZ, and WO_x/C catalysts were obtained by nitrogen adsorption-desorption measurements (BELSORP mini II). Before the analyses, all the catalysts were degassed using a rotary vacuum pump at 150 °C for 3 h to remove impurities and moisture. Surface morphologies of the catalyst were examined by FE-SEM (Scanning Electron Microscope) analyses (JSM-6700F, Jeol). To confirm the detailed distribution of metal species of the catalysts, energy dispersive X-ray spectroscopy (EDX) mapping analyses were conducted (JSM-6700F, Jeol). X-ray diffraction patterns of supports (Z, CZ, and C) and catalysts (WO_x/Z, WO_x/CZ, and WO_x/C) were taken with an X-ray diffractometer (Rigaku, D-MAX2500-PC) operated at 50 kV and 100 mA using Cu-Ka radiation (λ = 0.154056 nm). The acidity of the catalysts was measured by NH_3-TPD (Temperature Programmed Desorption) experiments (BEL Japan, BELCAT-B). In order to remove any physisorbed organic molecules, 0.05 g of each catalyst was treated in TPD apparatus at 200 °C for 2 h with a stream of helium (50 ml/min). After cooling the catalyst to 25 °C, NH_3 (50 ml) gas was then introduced into the reactor at room temperature in a stream of helium (30 ml/min) to saturate acid sites of the catalyst. Physisorbed ammonia was removed at 100 °C for 1 h under a flow of helium (50 ml/min). After cooling the catalyst, NH_3-TPD measurement was conducted within the temperature range of 50–600 °C under helium flow (50 ml/min). Thermal

conductivity detector (TCD) was used to detect desorbed NH_3. Basicity of the catalysts was measured by CO_2-TPD experiments. Experimental procedures for CO_2-TPD were identical to those for NH_3-TPD, except that CO_2 instead of NH_3 was employed as a probe molecule. Reduction behavior of supports (Z, CZ, and C) and catalysts (WO_x/Z, WO_x/CZ, and WO_x/C) were investigated by H_2-TPR (temperature programmed reduction) experiments using a conventional flow system equipped with a TCD (thermal conductivity detector) at temperatures ranging from 50 to 900 ^oC with a ramping rate of 10 ^oC/min under a mixed stream of H_2 (2 ml/min) and N_2 (20 ml/min). 50 mg of each catalyst was loaded into the U-shaped quartz reactor.

4.2.3. Catalytic reaction tests

The catalytic activity of WO_x/Z, WO_x/CZ, and WO_x/C catalysts in the propylene epoxidation by oxygen was evaluated in a continuous flow fixed-bed reactor at 400 ℃ for 6 h under atmospheric pressure. Prior to the catalytic reaction, each catalyst (0.3 g) was pretreated at 400 ℃ for 1 h with a nitrogen stream (45 ml/min). Feed stream of propylene (10 ml/min) and oxygen (5 ml/min) was continuously fed into the reactor together with nitrogen carrier (45 ml/min). Total feed rate with respect to catalyst weight was maintained at 12000 ml/h · g. Reaction products were periodically sampled and analyzed with gas chromatographs (Younglin, ACME 6100) equipped with a thermal conductivity detector (Molsieve 5A and Porapak N columns) and a flame ionization detector (DB-1 column). Conversion of propylene and selectivity for propylene oxide were calculated on the basis of carbon balance as follows. Yield for propylene oxide was calculated by multiplying conversion of propylene and selectivity for propylene oxide.

$$\text{Conversion of propylene (\%)} = \frac{\text{mole of propylene reacted}}{\text{mole of propylene supplied}} \times 100$$

$$\text{Selectivity for propylene oxide (\%)} = \frac{\text{mole of propylene oxide formed}}{\text{mole of propylene reacted}} \times 100$$

4.3. Results

4.3.1. Catalytic performance of ceria & zirconia-supported tungsten oxides

4.3.1.1. $WO_x/Ce_xZr_{1-x}O_2$ catalyst for the propylene epoxidation

Fig. 4-2 shows the effect of the Zr/Ce composition on the catalytic activity of the $WO_x/Ce_xZr_{1-x}O_2$ (x =0.05, 0.1, 0.2, 0.3, 0.4, and 0.5) catalysts at 400 ^oC. The tungsten loading was fixed at 7 wt% and the calcination temperature of the catalyst was 700 ^oC. It is clear that the propylene conversion and propylene oxide selectivity was markedly affected by the Zr/Ce mole ratio in the $WO_x/Ce_xZr_{1-x}O_2$ catalysts. WO_x/ZrO_2 catalyst without cerium showed high propylene oxide selectivity (61.2 %) but very low propylene conversion (0.19 %). As a result, a very low propylene oxide yield (0.1 %) is obtained in WO_x/ZrO_2. A introduction of small amount of cerium ($WO_x/Ce_{0.05}Zr_{0.95}O_2$) resulted in a significant increase of propylene oxide yield (from 0.1 % to 1.4 %). With an increase of cerium mole ratio from 0.05 to 0.5 in the $WO_x/Ce_xZr_{1-x}O_2$ catalyst, propylene conversion increased from 4.5 % to 24.7 %, while propylene oxide selectivity significantly decreased from 31.6 % to 2.7 %. When cerium mole ratio higher than 0.05, however, both propylene oxide selectivity and yield decreased. These results indicate that introduction of cerium is advantageous in terms of propylene conversion, and there is an optimum cerium content for desirable propylene oxide selectivity and yield.

4.3.1.2. Effect of (X wt%) $WO_x/Ce_{0.05}Zr_{0.95}O_2$ catalyst on the propylene epoxidation

Fig. 4-3 shows the effect of tungsten oxide loading on the catalytic performance of the (X wt%) $WO_x/Ce_{0.05}Zr_{0.95}O_2$ (X= 1.8, 3.6, 4.8, 7.0, 10.0, and 13.6) catalysts at 400 ^oC. The calcination temperature of the catalysts was 700 ^oC. At tungsten oxide loading less than 5 wt%, propylene conversion was very low. With an increase of tungsten oxide loading from 4.8 % to 7.0 %, the propylene conversion increased sharply from 0.87 % to 4.5 %, and then saturated. Meanwhile, the propylene oxide selectivity deceased slightly from 45.7 % to 31.6 %, and then remained constant in the range of 31 and 33 %. Among the samples, 10 wt% $WO_x/Ce_{0.05}Zr_{0.95}O_2$ catalyst exhibited the maximum propylene oxide selectivity of 33.8 % with propylene conversion of 5.2 %. This demonstrates the promotional effect of tungsten oxide on the production of propylene oxide over the $WO_x/Ce_{0.05}Zr_{0.95}O_2$ catalyst.

4.3.1.3. Effect of calcination temperature on the propylene epoxidation over (10 wt%) $WO_x/Ce_{0.05}Zr_{0.95}O_2$ catalyst

Fig. 4-4 shows the effect of calcination temperature on the catalytic performance of the (10 wt%) $WO_x/Ce_{0.05}Zr_{0.95}O_2$-*X* (X= 500, 600, 700, 800, and 900 ^oC) catalysts at 400 ^oC. It can be seen that propylene conversion and propylene oxide selectivity was greatly influenced by the calcination temperature of catalyst. The conversion of propylene decreased from 8.3 % to

0.19 % with increasing calcination temperature from 500 ^{o}C to 900 ^{o}C, whereas selectivity for propylene oxide increased from 20.4 % to 99.7 %, respectively. (10 wt%) $WO_x/Ce_{0.05}Zr_{0.95}O_2$-900 sample showed about 100% propylene oxide selectivity, while the propylene conversion was very low (0.19 %), leading to very low propylene oxide yield of 0.18 %. Therefore, a calcination temperature of 800 ^{o}C is regarded as the optimum to produce propylene oxide.

4.3.2. Characterization of ceria & zirconia-supported tungsten oxides

4.3.2.1. Textural properties and morphology of catalysts

In the previous section, (10 wt%) $WO_x/Ce_{0.05}Zr_{0.95}O_2$-800 catalyst was selected as an optimum catalyst in the production of propylene oxide. Further characterization and reaction experiments were performed with (10 wt%) $WO_x/Ce_{0.05}Zr_{0.95}O_2$-800 catalyst to understand the role of WO_x and ceria-zirconia support. For comparison, analysis of WO_x/ZrO_2 and WO_x/CeO_2 catalysts also were carried out in the same condition as that of $WO_x/CeZrO_2$ catalyst.

WO_x contents and Zr/Ce ratios in the WO_x/Z, WO_x/CZ, and WO_x/C catalysts determined by XRF analyses are listed in Table 4-1. Actual WO_x loading and Zr/Ce atomic ratios determined by XRF were close to the designed values (10 wt% WO_x and 19 Zr/Ce atomic ratio, respectively) for all catalysts prepared. All the prepared catalysts retained low BET surface area (< 30 m^2/g) and large average pore diameter (> 5 nm).

In order to confirm the morphology and the distribution of elements, FE-SEM and SEM-EDX mapping analyses were carried out. Fig. 4-5 shows the FE-SEM and SEM-EDX mapping images of WO_x/CZ catalyst. The FE-SEM image (a) of the catalyst clearly shows that uniform and bulk-type

particles with a diameter of ca. 300 nm were successfully formed. The elemental mapping images obtained for oxygen atom (green dot (c)), zirconium atom (red dot (d)), cerium atom (yellow dot (e)), and tungsten atom (purple dot (f)) were matched with the SEM image (b). The EDX mapping images of WO_x/CZ catalyst clearly showed that all elements were uniformly distributed in the catalyst.

Crystalline structures of supports and catalysts were confirmed by X-ray diffraction (XRD) measurements. Fig. 4-6(a) shows the XRD patterns of ZrO_2, $Ce_{0.05}Zr_{0.95}O_2$, and CeO_2 supports. We found that the ZrO_2 support exhibited the characteristic XRD peaks of monoclinic ZrO_2 ($2\theta = 28^o$ and 31^o) and tetragonal ZrO_2 ($2\theta = 30^o$) [38]. The CeO_2 support also showed four distinct diffraction peaks corresponding to CeO_2 cubic phase [54,55]. It is noticeable that the characteristic XRD peaks of $Ce_{0.05}Zr_{0.95}O_2$ support slightly shifted to higher angles compared to the peaks for cubic phase of CeO_2 support. It has been reported that the shift of XRD peaks was attributed to the ionic radius difference between Ce^{4+} (ionic radius=0.098 nm) and Zr^{4+} (ionic radius=0.084 nm) in the $Ce_{0.05}Zr_{0.95}O_2$ support [56]. Fig. 4-6(b) shows the XRD patterns of WO_x/Z, WO_x/CZ, and WO_x/C catalysts. All the catalysts showed the XRD peaks of tungsten oxide (WO_x) in the 2θ region of 23–25°. It was found that there is no significant difference in peak intensity of the catalysts. This indicate that highly crystalline tungsten oxide phase exists in all the catalysts. These results were well consistent with the result of previous work [57.58], indicating that WO_x/Z, WO_x/CZ, and WO_x/C catalysts were successfully prepared in this work.

4.3.2.2. H_2-TPR of catalysts

H_2-TPR experiment was carried out to elucidate the reduction behavior of supports (Z, CZ, and C) and catalysts (WO_x/Z, WO_x/CZ, and WO_x/C). Fig. 4-7(a) shows the TPR profiles of ZrO_2, $Ce_{0.05}Zr_{0.95}O_2$, and CeO_2 supports. Pure ZrO_2 support did not show any reduction peak within that temperature range, in good agreement the previous work [58-60]. On the other hand, pure CeO_2 support exhibited two reduction peaks at 495 ^oC and 830 ^oC in the TPR profile; the former was attributed to the reduction of the surface CeO_2, while the latter was attributed to that of the bulk CeO_2 [59-61]. In case of $Ce_{0.05}Zr_{0.95}O_2$ support, one peak at 640 ^oC was obseved from the reduction of (Ce-Zr)O_2 solid solution [59,60]. Fig. 4-7(b) shows the TPR profiles of WO_x/Z, WO_x/CZ, and WO_x/C catalysts. Since pure ZrO_2 support does not show a reduction peak, the reduction peaks of WO_x/Z catalyst are attributed to the reduction of WO_x. It is well known that pure WO_x shows three reduction peaks; a peak at around 500 ^oC is attributed to the reduction of WO_3 to $W_{20}O_{58}$; a peak at around 800 ^oC is the reduction of $W_{20}O_{58}$ to WO_2; a peak at higher temperature is the reduction of WO_2 to W [62,63]. In our TPR data, WO_x/Z catalyst showed three reduction peaks at 374 ^oC, 580 ^oC, 641 ^oC respectively. These three reduction peaks over zirconia-supported tunsten oxide catalyst were also reported by D.C. Calabro et al. [58]. WO_x/CZ and WO_x/C catalysts also exhibited three reduction peaks. In case of WO_x/CZ catalyst, peak temperatures slightly shifted to higher temperature and amount of H_2 consumption in the range of 600-650 ^oC increased compared to WO_x/Z catalyst. In addition, considering TPR profiles of CZ support and WO_x/CZ

catalyst, the peak at 395 ºC is regarded as the reduction peak of tungsten oxide, and the peak at around 600 ºC is expected to overlap with the reduction peak of tungsten oxide and CZ support. On the other hand, WO_x/C catalyst showed a large temperature shift and the amount of H_2 consumption at around 450 ºC and 800 ºC increased. This result is also attributed to the overlapping with the reduction of tungsten oxide and CeO_2 species. The amount of H_2 consumption was calculated from each peak area in the H_2-TPR profiles as summarized in Table 4-2. Considering the fact that our reaction experiments were conducted at 400 ºC, it is reasonable to consider the H_2 consumption of the samples up to 400 ºC, which is summarized in Table 4-2. The H_2 consumption up to 400 ºC were decreased in the order of WO_x/C (21.8 μmol H_2/g_{cat}) > WO_x/CZ (4.3 μmol H_2/g_{cat}) > WO_x/Z (1.4 μmol H_2/g_{cat}). The hydrogen consumption up to 400 ºC was significantly different, which is expected to affect the reaction activity.

4.3.3. Acidity & basicity of catalysts

In order to elucidate the effect of acid & base property on the catalytic activity of catalysts, NH_3-TPD and CO_2-TPD experiments were carried out, respectively. Fig. 4-8 shows the NH_3-TPD profiles of WO_x/Z, WO_x/CZ, and WO_x/C catalysts. WO_x/Z catalyst showed a broad ammonia desorption peak in the range of 50-600 ^oC, whereas WO_x/C catalyst showed a small NH_3-TPD profile. It is noteworthy that WO_x/CZ catalyst showed an intermediate NH_3-TPD profile between WO_x/Z and WO_x/C. This is explained by the fact that the introduction of Ce, which has no acid site, reduces the ammonia adsorption capacity of ZrO_2 [64]. Fig. 4-9 shows the CO_2-TPD profiles of WO_x/Z, WO_x/CZ, and WO_x/C catalysts. Contrary to acidity of the catalysts, WO_x/C catalyst showed a large CO_2 desorption peak, whereas WO_x/Z catalyst showed a small desorption. WO_x/CZ catalyst also showed an intermediate CO_2-TPD profile between WO_x/C and WO_x/Z. It is known that pure CeO_2 has larger carbon dioxide adsorption capacity than pure ZrO_2 [65]. Acidity and basicity of the catalysts obtained from NH_3-TPD peak area and CO_2-TPD peak area are summarized in Table 4-3. WO_x/Z catalyst showed the highest acidity (0.63 mmol NH_3/g_{cat}) and the lowest basicity (0.20 mmol CO_2/g_{cat}), although WO_x/C catalyst exhibited the lowest acidity (0.09 mmol NH_3/g_{cat}) and the highest basicity (0.75 mmol CO_2/g_{cat}). In case of WO_x/CZ catalyst, acidity and basicity were found to be intermediate value between WO_x/Z and WO_x/C catalysts.

4.3.4. Catalytic activity in the propylene epoxidation by oxygen

Fig. 4-10 shows the conversion of propylene and selectivity for propylene oxide with time on stream in the propylene epoxidation by oxygen over WO_x/Z, WO_x/CZ, and WO_x/C catalysts at 400 ^oC. All the catalysts showed a stable catalytic performance without any significant catalyst deactivation during the reaction. It must be also pointed out that all the catalysts exhibited a stable catalytic performance without any significant deactivation during the 24 h reaction activity test (these are not shown here). This result show that the stability of the reaction activity is improved as compared with the previously reported catalysts [47,48]. Catalytic performance after 6 h-catalytic reaction over supported WO_x/Z, WO_x/CZ, and WO_x/C catalysts is summarized in Table 4-4. For comparison, catalytic performance of supports (Z, CZ, and C) is also listed in Table 4-4. First, Z and CZ showed no catalytic activity. On the other hand, C support showed the conversion of propylene (27.5 %), but the selectivity for propylene oxide was 0 %. WO_x/Z catalyst showed the lowest conversion of propylene (0.57 %) and the highest selectivity for propylene oxide (99.4 %). In other words, selectivity for propylene oxide is superior on the pure ZrO_2 support, although the propylene conversion rarely occurs. Contrary to WO_x/Z catalyst, WO_x/C catalyst showed the highest conversion of propylene (38.5 %) and the lowest selectivity for propylene oxide (11.7 %). This means that the reacted propylene was mostly converted to CO and CO_2 on the pure CeO_2 support. Meanwhile, WO_x/CZ catalyst with ceria and zirconia showed the conversion

of propylene (3.8 %) and the selectivity for propylene oxide (46.8 %). The above results indicate that pure CeO_2 is advantageous for the conversion of propylene, whereas pure ZrO_2 is more efficient in terms of selectivity for propylene oxide.

4.4. Discussion

On the basis of the combined results described above, it was found that the physicochemical properties of catalysts were varied depending on type of support. In our TPR data, we could not observe any H_2 consumption at around 400 ^oC in Z and CZ supports. This indicates that propylene does not react with oxygen present in Z and CZ supports at the reaction condition. Actually, Z and CZ supports showed no catalytic activity in our reaction experiments. Tungsten oxide containing WO_x/Z and WO_x/CZ catalysts, however, exhibited the TPR peak at around 400 ^oC and showed a catalytic activity. Therefore, it is speculated that the oxygen of tungsten oxide reacts with propylene in the WO_x/Z and WO_x/CZ catalysts. On the other hand, CeO_2 support and WO_x/C catalyst showed a different behavior. Firstly, CeO_2 support showed a TPR peak in the range of 300-600 ^oC and exhibited about 20 % propylene conversion. In case of WO_x/C catalyst, a TPR peak in the range of 350-550 ^oC was also observed. However, the reaction products of CeO_2 support were primarily CO and CO_2, while WO_x/C catalyst showed about 11% propylene oxide selectivity. It means that CO and CO_2 are produced by the reaction between propylene and lattice oxygen of CeO_2 support, while propylene oxide is formed by the reaction between propylene and oxygen of tungsten oxide. For more detailed analysis, we have related propylene conversion and

hydrogen consumption up to 400 °C during H_2-TPR. As a result, the trend of propylene conversion (WO_x/Z (0.57 %) < WO_x/CZ (3.8 %) < WO_x/C (38.5 %)) was well matched with the trend of hydrogen consumption up to 400 °C (WO_x/Z (1.4 μmol H_2/g_{cat}) < WO_x/CZ (4.3 μmol H_2/g_{cat}) < WO_x/C (21.8 μmol H_2/g_{cat})). However, it must be pointed out that the selectivity for propylene oxide does not match this tendency. Even considering the hydrogen consumption ((WO_x/Z (1.4 μmol H_2/g_{cat}) < WO_x/CZ (4.3 μmol H_2/g_{cat}) < WO_x/C (9.2 μmol H_2/g_{cat})) of tungsten oxide, which is related to the production of propylene oxide, it does not match the selectivity for propylene oxide. Therefore, we paid attention to the acid/base properties of the catalysts.

We found that the acid/base properties were influenced by the type of support (ZrO_2, $CeZrO_2$, and CeO_2). Generally, in a silver catalyst system, acid site of catalyst makes adsorbed oxygen on silver more electrophilic by acting as an electron acceptor [18]. As a result, the possibility to proceed the reaction between propylene C=C π bond and adsorbed oxygen is increased, leading to the formation of propylene oxide. Meanwhile, acid-base reaction between basic site of catalyst and propylene allylic hydrogen occurred, resulting in the formation of CO_2 and H_2O [18]. In our previous work [66], it was also reported that acid site was beneficial to produce propylene oxide, whereas basic site was good for producing CO_2 and H_2O in Ag-(Mo-W)/ZrO_2 catalyst. Accordingly, in a silver catalyst system, electronic state of adsorbed oxygen on silver played a key role in determining the production of propylene oxide. The same argument might also be applied to tungsten oxide catalyst system.

Haber et al. reported that the electrophilic oxygen species in the metal oxide react with the π-bond of propylene, resulting in the formation of epoxy or peroxy complexes [67]. From the above experimental results, it can be inferred that oxygen of tungsten oxide, not oxygen of support, is involved in the formation of propylene oxide. Therefore, it may be speculated that acid site affects the electronic property of oxygen on tungsten oxide, which is involved in formation of propylene oxide, while basic site reacts with allylic hydrogen of propylene to form CO_2 and H_2O. Accordingly, we calculated the ratio of acidity/basicity from NH_3-TPD and CO_2-TPD peak area to investigate the effect of acidity and basicity on the propylene oxide production of WO_x/Z, WO_x/CZ, and WO_x/C catalysts. The calculated ratio of acidity/basicity is summarized in Table 4-3. It was found that the ratio of acidity/basicity increased in the order of WO_x/C (0.12) < WO_x/CZ (0.51) < WO_x/Z (3.15). Interestingly, the trend of ratio of acidity/basicity was well matched with the trend of selectivity for propylene oxide (WO_x/C (11.7 %) < WO_x/CZ (46.8 %) < WO_x/Z (99.4 %)). This result indicates that acid site can promote the reaction of olefinic carbon (C=C) with oxygen on tungsten oxide, whereas basic site facilitates the acid-base reaction of allylic hydrogen with basic site. Therefore, it is concluded that the oxygen involved in formation of propylene oxide is oxygen on tungsten oxide which is affected by the acid/base property of the catalyst.

Table 4-1. Textural properties of WO_x/Z, WO_x/CZ, and WO_x/C catalysts

Catalyst	S_{BET} (m^2/g)[a]	Average pore diameter (nm)[b]	WO_x content (wt %)	Zr/Ce atomic ratio
WO_x/Z	10.8	5.6	9.5 (10)[c]	-
WO_x/CZ	12.3	8.3	9.9 (10)[c]	19.2 (19)[d]
WO_x/C	16.2	6.7	9.7 (10)[c]	-

[a] Calculated by the BET (Brunauer–Emmett–Teller) equation
[b] BJH (Barret–Joyner–Hallender) desorption average pore diameter
[c] Designed values of WO_x contents in the WO_x/Z, WO_x/CZ, and WO_x/C catalysts
[d] Designed values of Zr/Ce ratios in the WO_x/CZ catalysts

Table 4-2. H_2 consumption of ZrO_2, $CeZrO_2$, and CeO_2 supports and WO_x/Z, WO_x/CZ, and WO_x/C catalysts

Support	Amount of H_2 consumption up to 400 °C (μmol H_2/g_{cat})	Peak temperature (°C)	Amount of H_2 consumption (μmol H_2/g_{cat})	Catalyst	Amount of H_2 consumption up to 400 °C (μmol H_2/g_{cat})	Peak temperature (°C)	Amount of H_2 consumption (μmol H_2/g_{cat})
ZrO_2	-	-	-	WO_x/Z	1.4	374	2.6
						580, 641	35.2
$CeZrO_2$	-	640	13.7	WO_x/CZ	4.3	395	8.3
						609, 650	49.3
CeO_2	12.6	495	98.6	WO_x/C	21.8	430	114.9
		830	60.5			790, 820	86.8

Table 4-3. Acidity, basicity, and ratio of acidity/basicity of WO_x/Z, WO_x/CZ, and WO_x/C catalysts

Catalyst	Acidity (mmol NH_3/g_{cat})[a]	Basicity (mmol CO_2/g_{cat})[b]	Ratio of acidity/basicity
WO_x/Z	0.63	0.20	3.15
WO_x/CZ	0.21	0.41	0.51
WO_x/C	0.09	0.75	0.12

[a] Determined by NH_3-TPD measurement
[b] Determined by CO_2-TPD measurement

Table 4-4. Catalytic performance of ZrO_2, $CeZrO_2$, and CeO_2 supports and WO_x/Z, WO_x/CZ, and WO_x/C catalysts

	Propylene conversion (%)	Propylene oxide yield (%)	Selectivity (%)			
			PO	CO_2	CO	By-products[a]
Z	-	-	-	-	-	-
CZ	-	-	-	-	-	-
C	27.5	-	-	72.3	27.7	-
WO_x/Z	0.57	0.56	99.4	-	-	0.6
WO_x/CZ	3.8	1.78	46.8	43.7	6.6	2.9
WO_x/C	38.5	4.5	11.7	61.6	25.4	1.3

[a] By-products = acetone + acetaldehyde + hydrocarbon

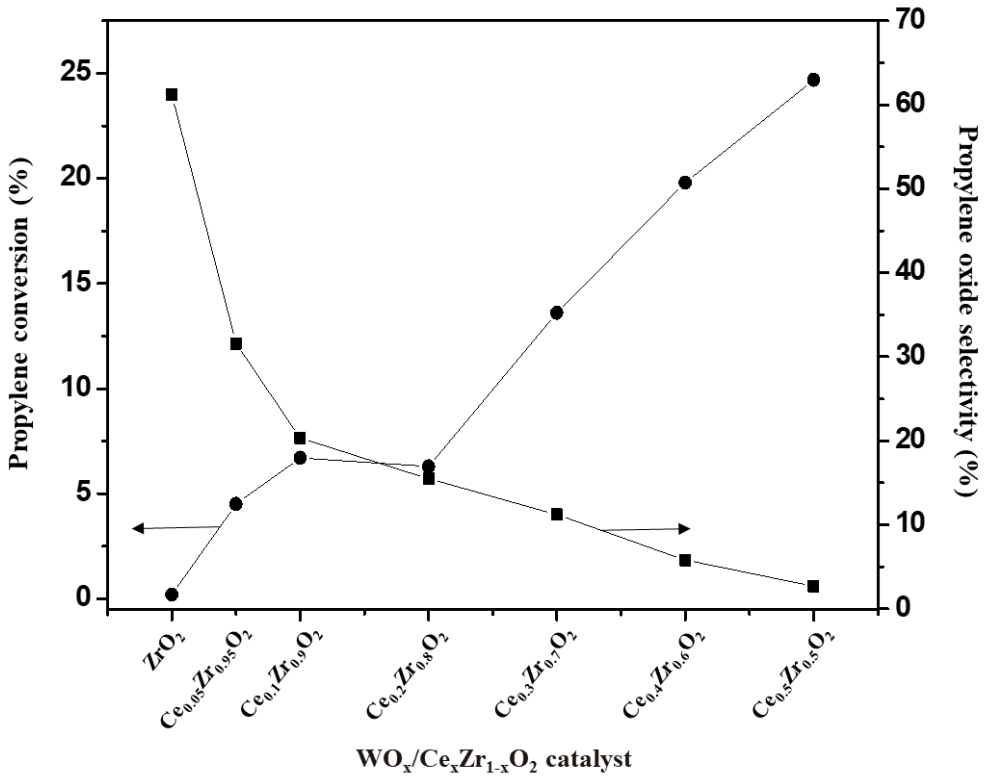

Fig. 4-2. Catalytic performance of the $WO_x/Ce_xZr_{1-x}O_2$ (x =0.05, 0.1, 0.2, 0.3, 0.4, and 0.5) catalysts in the propylene epoxidation by oxygen.

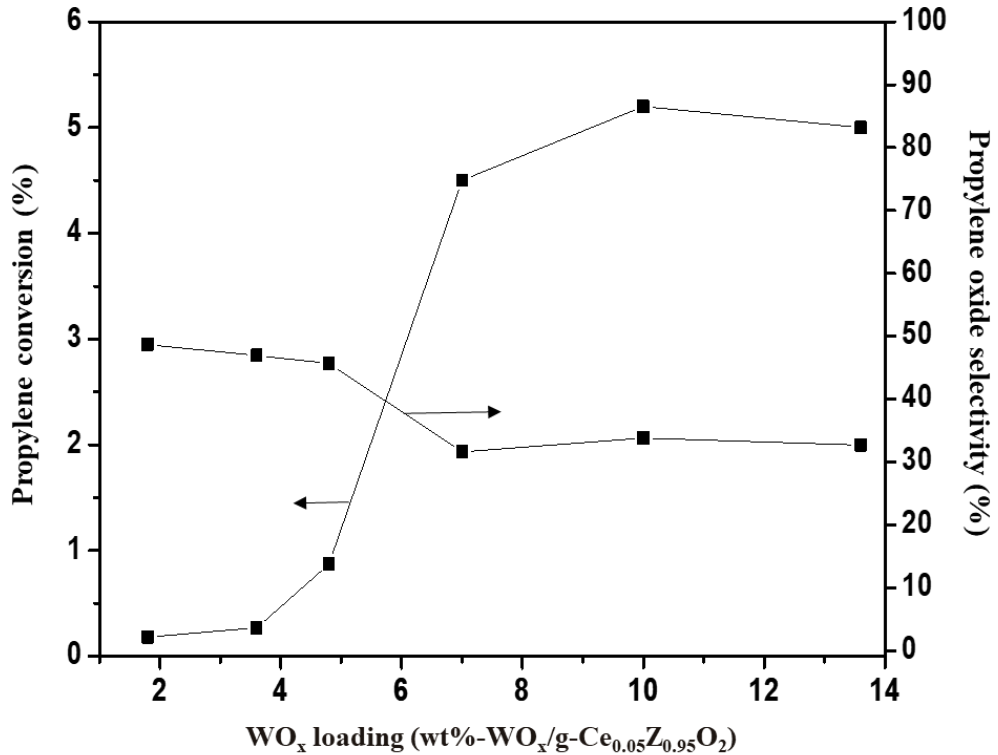

Fig. 4-3. Catalytic performance of the (X wt%) $WO_x/Ce_{0.05}Zr_{0.95}O_2$ (X= 1.8, 3.6, 4.8, 7.0, 10.0, and 13.6) catalysts in the propylene epoxidation by oxygen.

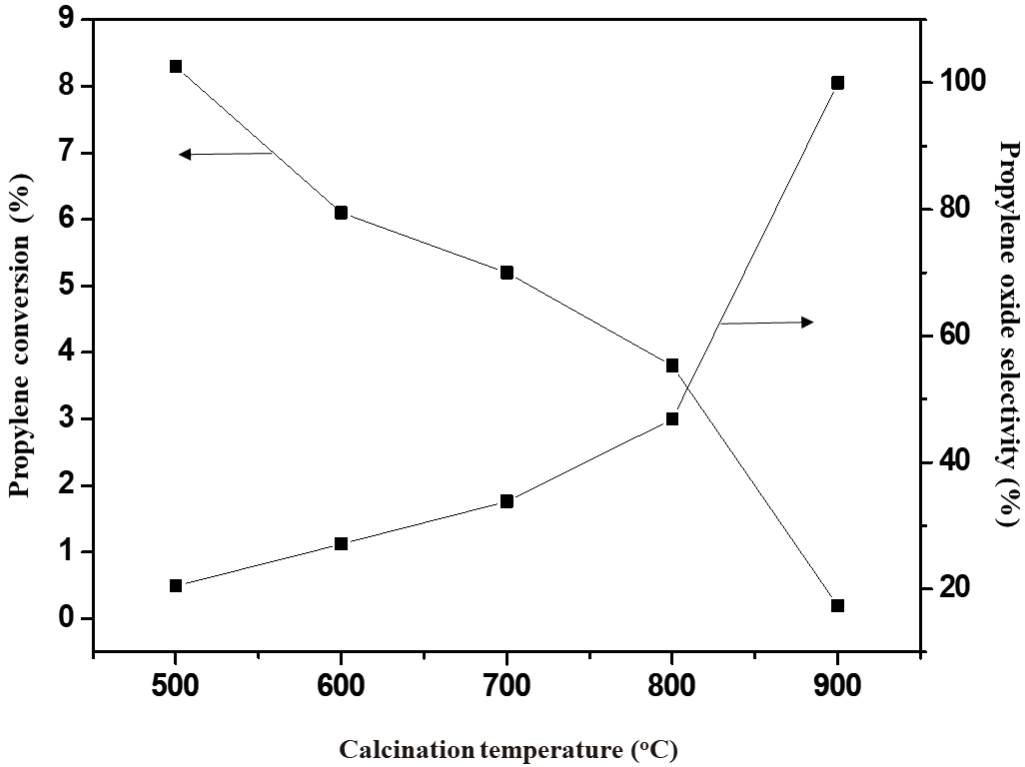

Fig. 4-4. Catalytic performance of the (10 wt%) WO_x/ $Ce_{0.05}Zr_{0.95}O_2$-*X* (*X*= 500, 600, 700, 800, and 900 °C) catalysts in the propylene epoxidation by oxygen.

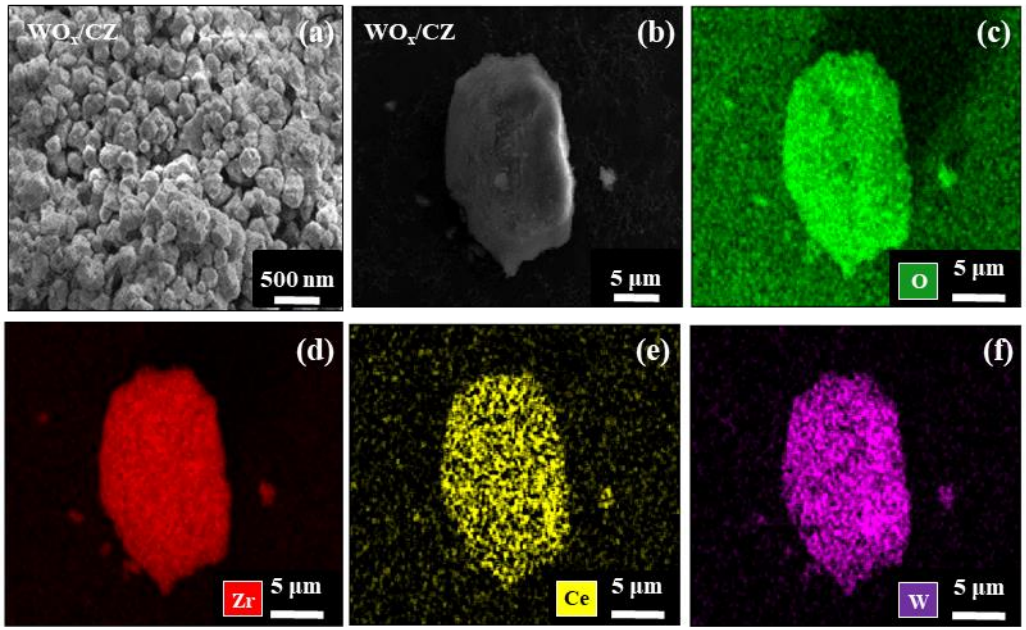

Fig. 4-5. FE-SEM and EDX mapping images of WO_x/CZ catalyst.

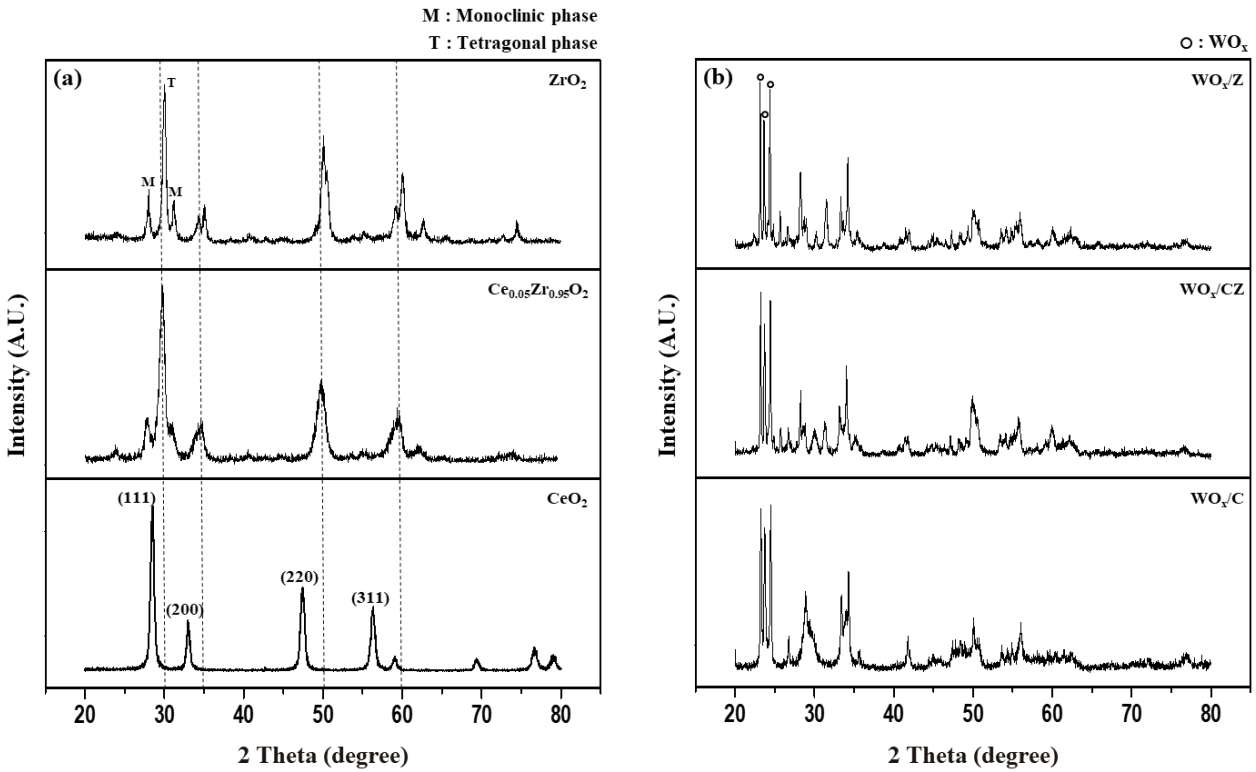

Fig. 4-6. (a) XRD patterns of ZrO_2, $Ce_{0.05}Zr_{0.95}O_2$, and CeO_2 supports, and (b) XRD patterns of WO_x/Z, WO_x/CZ, and WO_x/C catalysts.

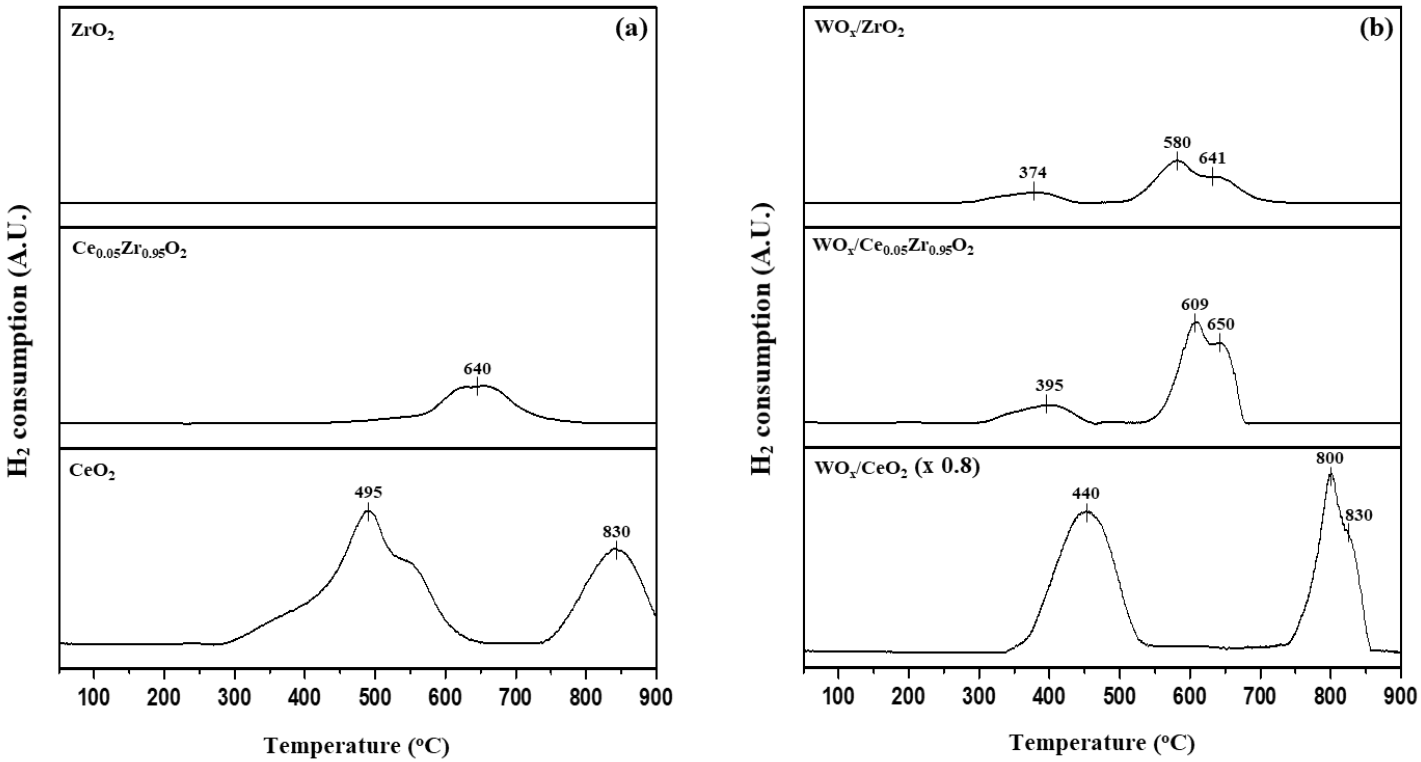

Fig. 4-7. (a) TPR profiles of ZrO_2, $Ce_{0.05}Zr_{0.95}O_2$, and CeO_2 supports, and (b) TPR profiles WO_x/Z, WO_x/CZ, and WO_x/C catalysts.

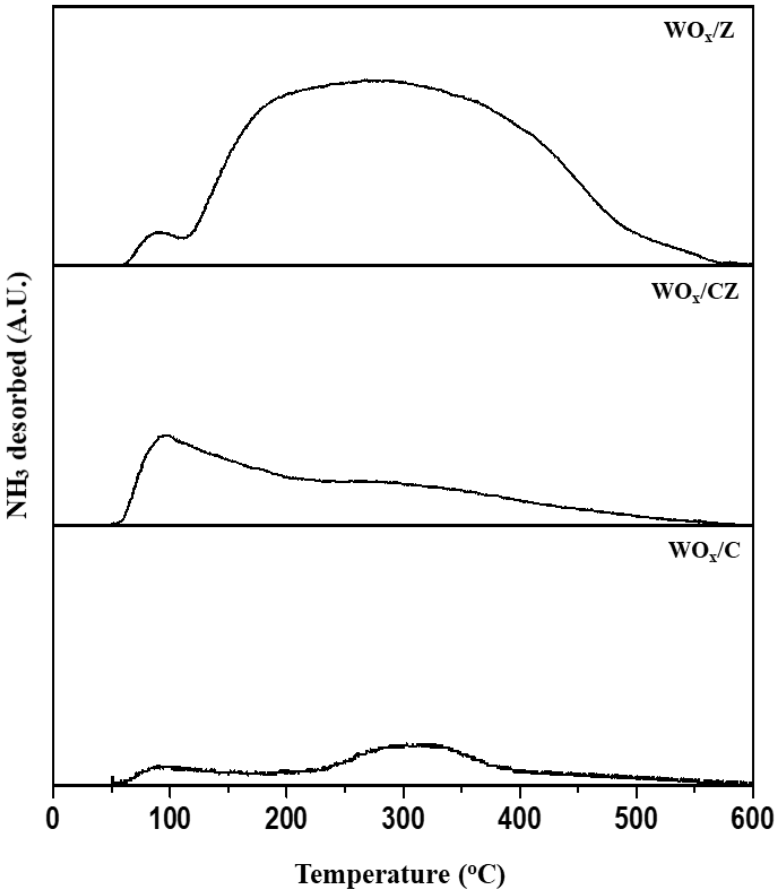

Fig. 4-8. NH_3-TPD profiles of WO_x/Z, WO_x/CZ, and WO_x/C catalysts.

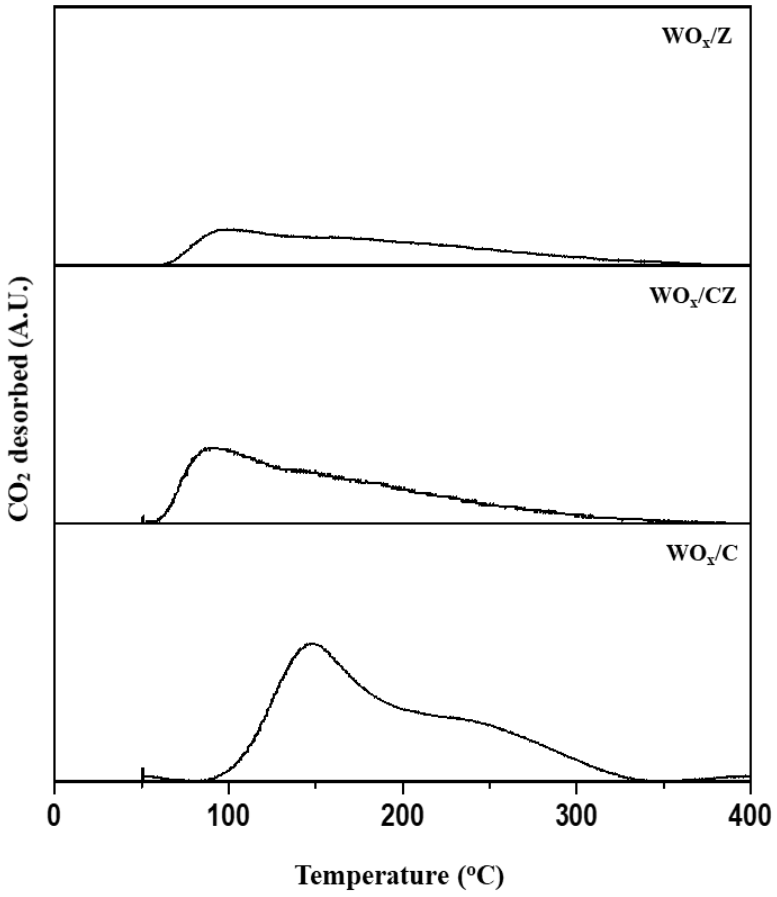

Fig. 4-9. CO_2-TPD profiles of WO_x/Z, WO_x/CZ, and WO_x/C catalysts.

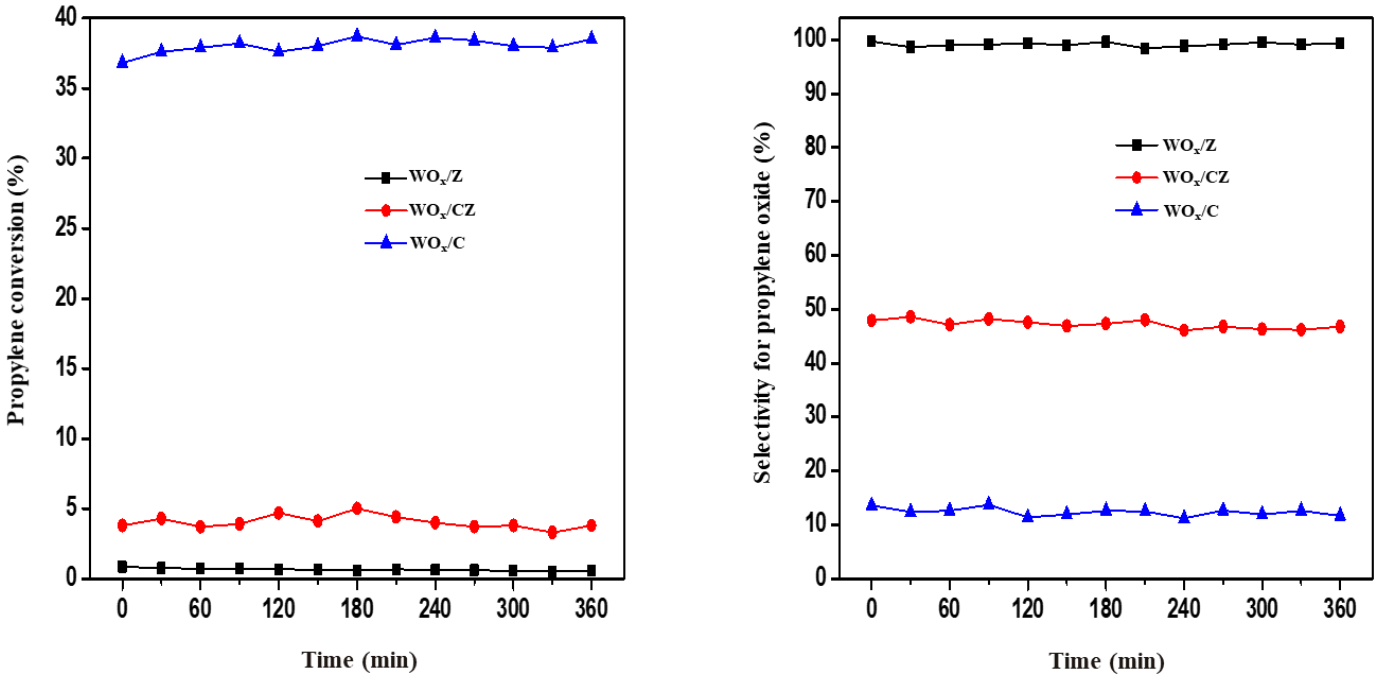

Fig. 4-10. Propylene conversion and propylene oxide selectivity with time on stream in the propylene epoxidation by oxygen over WO_x/Z, WO_x/CZ, and WO_x/C catalysts at 400 °C.

Chapter 5. Conclusions

A series of Ag-(x)Mo-(5-x)W/ZrO_2 (x = 5, 3.75, 2.50, 1.25, and 0) catalysts with different molybdenum content (x, wt%) were prepared by a slurry method for use in the direct epoxidation of propylene with molecular oxygen. The effect of molybdenum content on the physicochemical properties and catalytic activities of the catalysts was investigated. Successful preparation of Ag-(x)Mo-(5-x)W/ZrO_2 catalysts was well confirmed by ICP-AES and XRD analyses. Uniform distributions of silver, molybdenum, tungsten, and zirconium species were confirmed by SEM-EDX analyses. It was also found that binding energy shift of Ag $3d_{5/2}$ of the catalysts was different depending on molybdenum content. In the direct epoxidation of propylene to propylene oxide, selectivity for propylene oxide showed a volcano-shaped trend with respect to molybdenum content. It was revealed that selectivity for propylene oxide increased with increasing binding energy shift of Ag $3d_{5/2}$ of the catalysts, indicating that electronic property of silver played an important role in determining the catalytic performance in the reaction. Among the catalysts, Ag-(3.75)Mo-(1.25)W/ZrO_2 catalyst with the highest binding energy shift of Ag $3d_{5/2}$ served as the most efficient catalyst in the direct epoxidation of propylene to propylene oxide.

A series of ZrO_2 (pH X) (X = 3, 6, 10, 12, and 14) supports were prepared by a precipitation method with a variation of pH value (pH X) of ZrO_2 solution. Ag-(Mo-W)/ZrO_2 (pH X) catalysts were then prepared by a slurry method for use in the direct epoxidation of propylene to propylene

oxide with molecular oxygen. The effect of pH value of ZrO_2 solution on the catalytic performance and physicochemical property of the catalysts was investigated. It was found that BET surface area and pore volume of Ag-(Mo-W)/ZrO_2 (pH X) catalysts showed no significant difference. In the SEM-EDX mapping analyses, it was revealed that all metal species were uniformly distributed in the Ag-(Mo-W)/ZrO_2 (pH 10) catalyst. XRD, NH_3-TPD, and CO_2-TPD results showed that ZrO_2 crystalline phase and acid/base property of the catalysts were different depending on pH value of ZrO_2 solution. In the direct epoxidation of propylene to propylene oxide, selectivity for propylene oxide showed a volcano-shaped trend with respect to pH value of ZrO_2 solution. This trend was well consistent with the fraction of monoclinic phase and the ratio of acidity/basicity of the catalysts. Thus, ZrO_2 crystalline phase and acid/base property played important roles in determining the catalytic performance in the production of propylene oxide through direct epoxidation of propylene with molecular oxygen. Among the catalysts, Ag-(Mo-W)/ZrO_2 (pH 10) catalyst with the highest fraction of monoclinic phase and the highest ratio of acidity/basicity served as the most efficient catalyst in the direct epoxidation of propylene to propylene oxide.

WO_x/Z, WO_x/CZ, and WO_x/C catalysts were prepared to apply for the propylene epoxidation by oxygen. It was found that WO_x/Z catalyst exhibited the highest selectivity for propylene oxide. However, very low propylene conversion was observed over WO_x/Z catalyst, leading to low yield for propylene oxide. On the other hand, WO_x/C catalyst exhibited higher conversion of propylene than WO_x/Z, while WO_x/C showed low selectivity for propylene oxide. Among the catalysts, WO_x/CZ catalyst with moderate

reduction ability and ratio of acidity/basicity exhibited the desirable conversion of propylene and selectivity for propylene oxide. In addition, it was found that conversion of propylene is related to the reduction ability, while the selectivity of propylene oxide is affected by acid/base property of the catalyst.

Bibliography

[1] A.C. Fyyie, Chem. Ind. London 10 (1964) 384.

[2] R.B. Stobaugh, V.A. Calarco, R.A. Morris, L.W. Stroud, Hydrocarbon Process 52 (1973) 99.

[3] J. Sobczak, J.J. Ziolkowski, J. Molecular Catal. 13 (1981) 11.

[4] A. Tullo, Chem. Eng. News 82 (2004) 15.

[5] R. Meiers, W.F. Holderich, Catal. Lett. 59 (1999) 161.

[6] M.G. Clerici, G. Bellussi, U. Romano, J. Catal. 129 (1991) 159.

[7] C.S. Hong, N.G. Park, J.S. Shin, Y.C. Kim, Theories and Applications of Chem. Eng. 9 (2003) 2.

[8] R.A.V. Santen, C.P.M. Groo, J. Catal. 98 (1986) 530.

[9] J.G. Serafin, A.C. Liu, S.R. Seyedmonir, J. Mol. Catal. A: Chem. 131 (1998) 157.

[10] D. Lafarga, M. Juaied, C. Bondy, A. Varma, Ind. Eng. Chem. Res. 39, (2000) 2148.

[11] D. Sullivan, P. Hooks, M. Mier, W. Jaap, V. Hal, X. Zhang, Top. Catal. 38 (2006) 4.

[12] Z.M. Hu, H. Nakai, H. Nakatsuji, Surf. Sci. 401 (1998) 371.

[13] J. Sheima, A. Khatib, S.T. Oyama, Catal. Rev. Sci. Eng. 57 (2015) 1.

[14] H. Nakatsuji, Prog. Surf. Sci. 54 (1997) 1.

[15] P.V. Geenen, H.J. Boss, G.T. Pott, J. Catal. 77 (1982) 499.

[16] F.W. Zemichael, A. Palermo, M.S. Tikov, R.M. Lambert, Catal. Lett. 80 (2002) 93.

[17] G. Jin, G. Lu, Y. Guo, J. Wang, X. Lu, Catal. Lett. 87 (2003) 249.

[18] G. Jin, G. Lu, Y. Guo, J. Wang, X. Lu, Catal. Today 93 (2004) 173.

[19] J. Lu, J. Juan, B. Suarez, M. Haruta, S.T. Oyama, Appl. Catal. A 302 (2006) 283.

[20] Y.F. Lin, F.L. Liang, Cryst. Eng. Comm. 17 (2015) 678.

[21] T.A. Nijhuis, M. Makkee, J.A. Moulijn, B.M. Weckhuysen, Ind. Eng. Chem. Res. 45 (2006) 3447.

[22] S.J. Ainsworth, Chem. Eng. News 2 (1992) 9.

[23] M. Akimoto, K. Ichikawa, E. Echigoya, J. Catal. 76 (1982) 333.

[24] M.A. Barteau, R.J. Madix, J. Am. Chem. Soc. 105 (1983) 344.

[25] A. Palermo, A. Husain, M.S. Tikhov, R.M. Lambert, J. Catal. 207 (2002) 331.

[26] A.M. Gaffney, A.P. Khan, R. Pitchai, U.S. Patent 5,703,254 (1997).

[27] B. Cooker, A.M. Gaffney, J.D. Jewson, W.H. Onimus, U.S. Patent 5,965,480 (1999).

[28] J. Lu, M. Luo, H .Lei, C. Li, Appl. Catal. A: Gen. 237 (2002) 11.

[29] W. Yao, G. Lu, Y. Guo, Y. Wang, Z. Zhang, J. Mol. Catal. A: Chem. 276 (2007) 162.

[30] G. Jin, G. Lu, Y. Guo, J. Wang, X. Liu, W. Kong, X. Liu, Catal. Lett. 97 (2004) 191.

[31] G. Jin, G. Lu, Y. Guo, J. Wang, W. Kong, X. Lu, J. Mol. Catal. A: Chem. 232 (2005) 165.

[32] Y. Li, D. He, Y. Yuan, Z. Cheng, Q. Zhu, Fuel 81 (2002) 1611.

[33] Y. Nakano, T. Iizuka, H. Hattori, K. Tanabe, J. Catal. 57 (1979) 1.

[34] B.H. Davis, J. Am. Ceram. Soc. 67 (1984) C168.

[35] M.B. Harris, S.F. Simpson, R.J. Angelis, B.H. Davis, J. Mater. Res. 3 (1988) 787.

[36] R.C.R. Neto, M. Schmal, Appl. Catal. A: Gen. 450 (2013) 131.

[37] E.J. Lee, J. Lee, Y.-J. Seo, J.W Lee, Y. Ro, J. Yi, I.K. Song, Catal. Comm. 89 (2017) 156.

[38] Y.F. Lin, F.L. Liang, Cryst. Eng. Comm. 17 (2015) 678.

[39] Z. Xu, Y. Zheng, Y. Guo, W. Ye, P. Yang, Mat. Res. 18 (2015) 146.

[40] N. Agasti, N.K. Kaushik, Am. J. Nanomater. 2 (2014) 4.

[41] H. Nakatsuji, H. Nakai, Can. J. Chem. 70 (1992) 404.

[42] T. Hayashi, K. Tanaka, M. Haruta, J. Catal. 178 (1998) 566.

[43] M. Akimoto, K. Ichikawa, E. Echigoya, J. Catal. 76 (1982) 333.

[44] J.G. Aguilar, I.M. Garcia, J.J. Juan, I.S. Basanez, E.S. Fabian, D.C. Amoros, A.B. Murcia, J. Catal. 338 (2016) 154.

[45] S. Ghosh, S.S. Acharyya, R. Tiwari, B. Sarkar, R.K. Singha, C. Pendem, T. Sasaki, R. Bal, ACS Catal. 4 (2014) 2169.

[46] H. Chu, L. Yang, Q. Zhang, Y. Wang, J. Catal. 241 (2006) 225.

[47] G.L. Montrasi, G.R. Tauszik, M. Solari, G. Leofanti, Appl. Catal. 5 (1983) 359.

[48] G. Boskovic, D. Wolf, A. Brückner, M. Baerns, J. Catal. 224 (2004) 187.

[49] L. Yang, J. He, Q. Zhang, Y. Wang, J. Catal. 276 (2010) 76.

[50] Z. Song, N. Mimura, J.J. Bravo-Suarez, T. Akita, S. Tsubota, S.T. Oyama, Appl. Catal. A: Gen. 316 (2007) 142.

[51] A. Bordoloi, N.T. Mathew, B.M. Devassy, S.P. Mirajkar, S.B. Halligudi, J. Mol. Catal. A: Chem. 247 (2006) 58.

[52] Z. Hasan, J. Jeon, S.H. Jhung, J. Hazard. Mater. 205 (2012) 216.

[53] L.F.R. Verduzco, J.A.D. Reyes, E.T. Garcia, Ind. Eng. Chem. Res. 47 (2008) 5353.

[54] T. Nakatani, H. Okamoto, J. Sol-Gel Sci. Technol. 26 (2003) 859.

[55] Z. Cui, J. Fan, H. Duan, J. Zhang, Y. Xue, Y. Tan, Korean J. Chem. Eng. 34 (2017) 29.

[56] G.R. Rao, T. Rajkumar, J. Colloid Interface Sci. 324 (2008) 134.

[57] V.C. Santosa, K. Wilsonb, A.F. Leeb, S. Nakagakia, Appl. Catal. B-Environ. 162 (2005) 75.

[58] D.C. Calabro, J.C. Vartuli, J.G. Santiesteban, Top. Catal. 18 (2002) 231.

[59] R.L. Oliveira, I.G. Bitencourt, F.B. Passos, J. Braz. Chem. Soc. 24 (2013) 68.

[60] P. Biswas, D. Kunzru, Int. J. Hydrogen Energy 32 (2007) 969.

[61] J. Kim, Y. Ryou, G. Hwang, J. Bang, J. Jung, Y. Bang, D.H. Kim, Korean J. Chem. Eng. 35 (2018) 2185.
[62] D.C. Vermaire, P.C.V. Berge, J. Catal. 116 (1989) 309.
[63] X.R. Chen, C.L. Chen, N.P. Xu, C.Y. Mou, Catal. Today 93 (2004) 129.
[64] B. Shen, X. Zhang, H. Ma, Y. Yao, T. Liu, J. Environ. Sci. 25 (2013) 791.
[65] D. Martin, D. Duprez, J. Phys. Chem. 100 (1996) 9429.
[66] E.J. Lee, J.W. Lee, J. Lee, H.K. Min, J. Yi, I.K. Song, D.H. Kim, Catal. Comm. 111 (2018) 80.
[67] J. Haber, W. Turek, J. Catal. 190 (2000) 320.

초 록

산화프로필렌의 석유화학산업에서 매우 큰 비중을 차지하고 있으며, 생산되는 프로필렌의 약 10 %가 산화프로필렌의 제조에 이용되고 있다. 산화프로필렌은 폴리우레탄의 원료가 되는 Polyether Polyol 및 Propylene Glycol 등의 제조에 원료로 쓰이고 있으며, 특히 Polyol에 사용되는 수요가 전체의 65%로 가장 많은 양을 차지한다. Polyether Polyol 및 Propylene Glycol은 Polyurethane의 제조에 이용되고 있으며, 그 수요가 증가하고 있어 산화프로필렌의 수요 또한 증가하고 있다. 현재 상업적으로 산화프로필렌은 대부분 간접 산화 공법 (chlorohydrin process and Halcon process) 을 통하여 제조되고 있다. 그러나 이러한 간접 산화 공법들은 환경 및 경제적 문제들을 수반한다. Chlorohydrin 공법은 염소를 사용하여 하이포아염소산을 만들고 이를 프로필렌과 반응시켜 Chlorohydrin 형태 화합물을 중간체로 하여 높은 수율의 산화프로필렌을 합성하는데, 부산물로 염화칼슘이 발생하며 용매로 많은 양의 용수가 쓰이는 단점이 있다. Halcon 공법은 원료의 종류에 따라 크게 2가지로 나뉘는데, 에틸벤젠을 반응물로 사용하여 부산물로 스티렌이 발생하는 PO-SM 공법과 이소부탄을 반응물로 사용하고 부산물로 tert-Butyl Alcohol이 발생하는 PO-TBA 공법으로 나눌 수 있다. 하지만, 본 공법들 역시 부산물로 발생하는 스티렌/알코올과 산화프로필렌의 분리·정제 공정이 요구되며 해당 부산물의 재활용 혹은 판매선의 확보가 필요하다는 단점이 있다. 한편, 이러한 공법들의 문제점들을 해결하기 위하여 과산화수소를 원료로 산화프로필렌을 생산하는

HPPO 공법이 개발되었다. HPPO 공법은 부산물로 물만 발생하여 친환경적 공법이지만, 반응물로 이용되는 과산화수소의 높은 비용 문제로 인하여 많은 양의 산화프로필렌을 생산하는데 한계가 있다. 따라서, 추가의 반응물을 이용하지 않고 프로필렌과 산소의 산화반응을 통해 산화프로필렌을 직접 제조하는 공정이 주목받고 있다. 먼저 프로필렌의 산화반응에서는 2 가지 경쟁반응이 존재하는데, 먼저 물과 이산화탄소가 생성되는 완전 산화 반응 ($C_3H_6 + 9/2O_2 \rightarrow 3CO_2 + 3H_2O$, $\Delta G = -1957.43$ kJ/mol)과 산화프로필렌이 생성되는 부분 산화 반응 ($C_3H_6 + 1/2O_2 \rightarrow 3C_3H_6O$, $\Delta G = -88.49$ kJ/mol)이 일어난다. 위 반응식에서 보여지는 것처럼 완전 산화반응은 부분 산화반응보다 열역학적인 측면에서 훨씬 안정적이기 때문에, 촉매의 개입이 없이는 프로필렌과 산소가 반응할 시 대부분 완전산화반응이 일어나게 되어 산화프로필렌의 생산이 어렵다는 것을 알 수 있다.

프로필렌의 직접 산화반응에서 산화프로필렌의 생성이 어렵다는 것은 산화 메커니즘에서도 알 수 있다. 본 반응에서 산화프로필렌이 생성되기 위해서는 금속에 흡착된 산소가 이중결합에 위치한 탄소와 반응하여 부분 산화반응이 일어나야 한다. 하지만, 프로필렌의 메틸기에 존재하는 allylic 수소의 반응성이 매우 크기 때문에, 금속에 흡착된 산소와 allylic 수소와의 반응을 통한 CO_2와 H_2O가 생성되는 완전 산화반응이 주로 일어나게 된다. 따라서 본 연구에서는 금속에 흡착된 산소가 프로필렌의 메틸기에 존재하는 allylic 수소와 반응하지 않고, 이중결합에 위치한 탄소와 선택적으로 반응시키는 것이 핵심이며, 이를 위하여 흡착된 산소의 전자적 성질은 전자친화적으로 변화시켜야 한다. 따라서 본

학위논문에서는 흡착된 산소의 전자적 성질을 변화시키기 위하여 Ag/ZrO_2 촉매에 몰리브덴과 텅스텐의 증진제를 도입하여 산화프로필렌 생산 효율을 최대화하였다.

다양한 몰리브덴 함량 (x = 5, 3.75, 2.50, 1.25, and 0 wt%)에 따라 일련의 $Ag-(x)Mo-(5-x)W/ZrO_2$ 촉매들을 슬러리 방법에 의해 제조하였다. $Ag-(x)Mo-(5-x)W/ZrO_2$ 촉매를 통한 프로필렌의 직접 산화반응에서 몰리브덴의 함량이 반응활성에 미치는 영향이 조사되었다. 그 결과, 몰리브덴의 함량에 따라 Ag의 바인딩 에너지 (Ag $3d_{5/2}$) 차이가 변화함을 확인하였다. 또한, 산화프로필렌의 선택도는 몰리브덴의 함량에 따라 화산형 경향을 나타내었다. 실험결과, 산화프로필렌의 선택도는 Ag의 바인딩 에너지 (Ag $3d_{5/2}$) 차이가 증가함에 따라 증가하는 것을 확인할 수 있었다. 따라서, 산화프로필렌의 선택도를 향상시키기 위해서는 은의 전자 상태가 중요한 요인임을 알 수 있으며, 또한 몰리브덴(Mo)과 텅스텐(W) 증진제가 이러한 역할을 수행함을 확인할 수 있다.

프로필렌의 직접 산화반응에서 보다 더 높은 효율의 촉매를 개발하기 위하여, 알칼리 토금속, $\alpha-Al_2O_3$, SiO_2와 같은 다양한 담체들에 은이 담지된 촉매가 연구되고 있다. 한편, 프로필렌의 직접 산화반응에서 담체 물질의 결정구조와 산/염기 특성이 산화프로필렌의 생산에 영향을 미치게 되며, ZrO_2를 제조 시 합성 조건의 변화에 따라 ZrO_2의 물리화학적 특성이 변화한다는 연구 결과들이 존재한다. 따라서, 본 학위 논문에서는 ZrO_2의 물리화학적 특성이 프로필렌의 직접 산화반응에 어떠한 영향을 미치는지 알아보기 위하여, ZrO_2 담체를 침전법으로 제조 시 pH 조건을

변화시켜 보았다.

다양한 pH 조건 (X = 3, 6, 10, 12, and 14)에 따라 일련의 ZrO_2 (pH X) 담체들을 침전법에 의해 제조하였다. 그 이후, 일련의 Ag−(Mo−W)/ZrO_2 (pH X) (X = 3, 6, 10, 12, and 14) 촉매들을 슬러리 방법을 통해 제조하였고, 이를 프로필렌의 직접 산화반응에 적용시켜, ZrO_2 담체 제조 시 pH 조건이 반응활성에 미치는 영향이 조사되었다. 실험결과, Ag−(Mo−W)/ZrO_2 (pH X) 촉매의 물리화학적 특성은 ZrO_2 담체 제조 pH에 의해 강하게 영향을 받았다. ZrO_2 담체 제조 pH에 따라 monoclinic 상의 비율과 산점/염기점 비율이 화산형 경향을 나타내는 것을 확인하였다. 또한, 프로필렌의 직접 산화반응에서, Ag−(Mo−W)/ZrO2 (pH X) 촉매의 monoclinic 상의 비율과 산점/염기점 비율은 산화프로필렌의 선택도와 밀접하게 관련이 있었다. 산화프로필렌의 선택도는 monoclinic 상의 비율과 산점/염기점 비율이 증가함에 따라 증가하였다. 따라서, 산화프로필렌의 선택도를 향상시키기 위해서는 촉매의 결정 구조와 산점/염기점 특성이 중요한 역할임을 알 수 있다.

프로필렌의 직접 산화반응을 위한 촉매연구들은 Ag 기반의 촉매들이 대부분 연구되어 왔다. 하지만, 상용 Ag 기반의 촉매들은 산화반응 상에서 Ag 입자들의 소결현상으로 인해 반응안정성이 떨어지게 된다. 또한, 높은 산화프로필렌 활성을 위해 많은 Ag 함량이 요구되어 역시 반응안정성의 감소를 야기한다. 이러한 이유로 최근 Ag을 대체할 수 있는 금속 산화물 촉매들이 연구되고 있다. 따라서, 본 학위 논문에서는 텅스텐 산화물을 다양한 담체 (ZrO_2, $CeZrO_2$, CeO_2)들에 담지시켜 프로필렌 직접 산화반응에

미치는 영향을 알아보았다.

$Ce_{0.05}Zr_{0.95}O_2$ (CZ) 담체는 침전법을 통해 제조하였다. 비교를 위해, ZrO_2 (Z)와 CeO_2 (C) 담체들 또한 동일한 조건으로 제조하였다. 그 이후, WO_x/Z, WO_x/CZ, WO_x/C 촉매들을 습윤함침법을 통해 제조하였고, 이들을 프로필렌 직접 산화반응에 적용시켜 보았다. 실험결과, WO_x/Z 촉매에서 가장 높은 산화프로필렌 선택도를 보였지만, 매우 낮은 프로필렌 전환율로 인하여 매우 낮은 산화프로필렌 수율을 나타내었다. 이와 대조적으로, WO_x/C 촉매는 높은 프로필렌 전환율을 보였지만, 낮은 산화프로필렌 선택도를 나타내었다. 제조된 촉매들 중 적절한 환원 능력과 산점/염기점 비율을 보인 WO_x/CZ 촉매에서 이상적인 프로필렌 전환율과 산화프로필렌 선택도를 나타내었다. 따라서, 프로필렌의 직접 산화반응에서 촉매의 환원 능력과 산점/염기점 비율이 반응활성에 중요한 요인임을 알 수 있다.

주요어: 프로필렌 직접 산화반응, 산화프로필렌, 은 촉매, 텅스텐 산화물 촉매

학 번: 2016-30235

List of publications

Papers

1. International Journal (First Author)

1. E.J. Lee, Y.J. Lee, J.K. Kim, U.G. Hong, J. Yi, J.R, Yoon, I.K. Song, *"CO_2 activated carbon aerogel with enhanced electrochemical performance as a supercapacitor electrode material"*, Journal of Nanoscience and Nanotechnology 15, pp.8917-8921 (2015).

2. E.J. Lee, Y.J. Lee, J.K. Kim, M. Lee, J. Yi, J.R, Yoon, I.K. Song, *"Oxygen group-containing activated carbon aerogel as an electrode material for supercapacitor"*, Materials Research Bulletin, 70, pp.209-214 (2015).

3. E.J. Lee, Y.J. Lee, J.K. Kim, M. Lee, J. Yi, J.R, Yoon, I.K. Song, *"Preparation and Characterization of Nitrogen-enriched Carbon Aerogel as a Supercapacitor Electrode Material"*, Journal of Nanoscience and Nanotechnology 16, pp.10413-10419 (2016).

4. E.J. Lee, J. Lee, Y.-J. Seo, Y. Ro, J. Yi, I.K. Song, *"Direct epoxidation of propylene to propylene oxide with molecular oxygen over Ag-Mo-W/ZrO_2 catalysts"*, Catalysis Communications, 89, pp.156-160 (2017).

5. E.J. Lee, J. Lee, Y.-J. Seo, Y. Ro, J. Yi, I.K. Song, *"Direct Epoxidation of Propylene to Propylene Oxide Over Ag-W/ZrO_2 Catalysts: Effect of Tungsten (W) Addition"*, Journal of Nanoscience and Nanotechnology 17, pp.8219-8225 (2017).

6. E.J. Lee, J.W. Lee, J. Lee, H.-K. Min, J. Yi, I.K. Song, D.H. Kim *"Ag-(Mo-W)/ZrO_2 catalysts for the production of propylene oxide: Effect of pH in the preparation of ZrO_2 support"*, Catalysis Communications 111, pp.80-83 (2018).

2. International Journal (Co-Author)

1. Y.J. Lee, J. Lee, G.-P. Kim, E.J. Lee, J. Yi, I.K. Song, *"Graphene-containing carbon aerogel prepared using polyethyleneimine (PEl)-modified graphene oxide (GO) for supercapacitor: effect of polyethyleneimine-modified GO content."*, Journal of Nanoscience and Nanotechnology 14, pp.8602-8608 (2014).

2. J.W. Lee, J.K. Kim, T.H. Kang, E.J. Lee, I.K. Song, *"Direct synthesis of hydrogen peroxide from hydrogen and oxygen over palladium catalyst supported on heteropolyacid-containig ordered mesoporous carbon"*, Catalysis Today, 293, pp.49-55 (2017).

3. S. Park, J. Y, S.J. Han, J.H. Song, E.J. Lee, I.K. Song, *"Steam reforming of liquefied natural gas (LNG) for hydrogen production over nickel–boron–alumina xerogel catalyst"*, International Journal of Hydrogen Energy 42, pp.15096-15106 (2017).

4. S. Park, S.J. Han, J. Yoo, J.H. Song, E.J. Lee, I.K. Song, *"Hydrogen Production by Steam Reforming of Liquefied Natural Gas (LNG) over Nickel-iron-alumina Aerogel Catalyst"*, Journal of Nanoscience and Nanotechnology 17, pp.8248-8254 (2017).

5. Y. Ro, M.Y. Gim, J.W. Lee, E.J. Lee, I.K. Song, *"Alkylation of Isobutane/2-Butene over Modified FAU-type Zeolites"*, Journal of Nanoscience and Nanotechnology 18, pp.6547-6551 (2018).

3. 특허

1. 이어진, 이중원, 민형기, 서영종, 송인규, 이종협, “프로필렌 직접산화 반응용 촉매, 이의 제조방법 및 이를 이용한 프로필렌 직접 산화반응에 의한 프로필렌 옥사이드 제조방법”, 대한민국 특허출원 10-2016-0106152 (2016).

2. 이어진, 이중원, 서영종, 송인규, 이종협, “프로필렌 직접산화반응 촉매용 지지체 및 이를 포함하는 프로필렌 직접산화 반응용 촉매” 대한민국 특허출원 10-2017-0117784 (2017).

3. J. Lee, Y.-J. Seo, J.R. I.K. Song, E.J. Lee, J. Yi, “Catalyst for direct oxidation of propylene to propylene oxide, preparing method same and preparing method of propylene oxide by direct oxidation of propylene using same” PCT/KR2017/009147 (2017).

4. International Conference (First Author)

1. E.J. Lee, Y.J. Lee, J.K. Kim, U.G. Hong, J. Yi, J.R. Yoon, I.K. Song, *"CO_2 Activated Carbon Aerogel with Enhanced Electrochemical Performance as a Supercapacitor Electrode Material"*, NANO Korea 2014 Symposium, P1406_003, Coex, Seoul, Korea (2014/7/2-4).

2. E.J. Lee, Y.J. Lee, J.K. Kim, M. Lee, J. Yi, J.R, Yoon, I.K. Song, *"Preparation and Characterization of Nitrogen-enriched Carbon Aerogel as a Supercapacitor Electrode Material"*, NANO Korea 2015 Symposium, P1506_100, Coex, Seoul, Korea (2015/7/1-3).

3. E.J. Lee, J. Lee, Y.-J. Seo, Y. Ro, J. Yi, I.K. Song, *"Direct Epoxidation of Propylene to Propylene Oxide Over Ag-W/ZrO_2 Catalysts: Effect of Tungsten (W) Addition"*, NANO Korea 2016 Symposium, P1605_0542, Kintex, Korea (2016/7/13-15).

5. International Conference (Co-Author)

1. J.W. Lee, J.K. Kim, T.H. Kang, E.J. Lee, I.K. Song, *"Direct synthesis of hydrogen peroxide from hydrogen and oxygen over palladium catalyst supported on heteropolyacid-containig ordered mesoporous carbon"*, The International Symposium on Catalytic Conversion of Energy and Resources 2016, GO B01, KOFST, Seoul, Korea (2016/6/30-7/2).

2. S. Park, T.H. Kim, E.J. Lee, S.J. Han, J. Yoo, J.H. Song, I.K. Song, *"Mesoporous Nickel-iron-alumina Catalysts for Hydorgen Production by Steam Reforming of Liquefied Natural Gas (LNG)"*, The 16th International Congress on Catalysis, PC066, Beijing, China (2016/7/3-8).

3. T.H. Kim, S. Park, K.H. Kang, E.J. Lee, W.C. Choi, Y.-K. Park, U.G. Hong, D.S. Park, C.-J. Kim, I.K. Song, *"Oxidative dehydrogenation of propane to propylene with lattice oxygen over CrO_y-CeO_2-K_2O/γ-Al_2O_3 catalysts"*, The 16th International Congress on Catalysis, PC109, Beijing, China (2016/7/3-8).

4. S. Park, S.J. Han, J. Yoo, J.H. Song, E.J. Lee, I.K. Song, *"Hydrogen Production by Steam Reforming of Liquefied Natural Gas (LNG) over Nickel-iron-alumina Aerogel Catalyst"*, NANO Korea 2016 Symposium, P1605_0546, Kintex, Korea (2016/7/13-15).

5. Y. Ro, M.Y. Gim, J.W. Lee, E.J. Lee, I.K. Song, *"Alkylation of Isobutane/2-Butene over Modified FAU-type Zeolites"*, NANO Korea 2017 Symposium, P1705_0012, Kintex, Korea (2017/7/12-14).

6. Domestic Conference (First Author)

1. 이어진, 이윤재, 김정권, 윤중락, 송인규, “카본 에어로젤의 표면 개질반응을 통한 슈퍼커패시터 전극용 활성 카본 에어로젤의 제조에서 카본 표면에 도입된 기능기와 커패시턴스의 관계 고찰”, 2014 년 한국화학공학회 추계학술회의, P 촉매금-10, 대전 DCC (2014/10/22-24).

2. 이어진, 이윤재, 김정권, 윤중락, 이종협, 송인규, “멜라민을 이용한 슈퍼커패시터 전극용 질소 도핑 카본 에어로젤의 제조에서 카본 표면에 도입된 질소 원자와 커패시턴스의 관계 고찰”, 2015 년 한국화학공학회 춘계학술회의, P 촉매목-8, 제주 ICC (2015/4/22-24).

3. 이어진, 이중원, 서영종, 이종원, 노영수, 이종협, 송인규, “몰리브덴 및 텅스텐 옥사이드 증진제를 포함하는 지르코늄 지지화은 촉매 상에서 프로필렌 직접산화 반응을 통한 프로필렌 옥사이드의 제조”, 2016 년 한국화학공학회 추계학술회의, P 촉매금-83, 대전 DCC (2016/10/19-21).

4. 이어진, 이중원, 서영종, 이종원, 노영수, 이민재, 이종협, 송인규, “침전법으로 제조된 지르코늄 옥사이드에 담지된 은 촉매 상에서의 프로필렌 직접산화 반응을 통한 프로필렌 옥사이드의 제조” 2017 년 한국화학공학회 춘계학술회의, P 촉매목-1, 제주 ICC (2017/4/26-28).

5. 이어진, 이중원, 서영종, 이종원, 노영수, 이종협, 송인규, “침전법으로 제조된 지르코늄 옥사이드에 담지된 은 촉매 상에서의 프로필렌 직접산화 반응을 통한 산화프로필렌의 제조” 2017 년 한국화학공학회 추계학술회의, P 촉매목-8, 대전 DCC (2017/10/25-27).

6. 이어진, 이중원, 민형기, 김도희, “침전법으로 제조한 산화지르코늄 담체에 담지된 은 촉매 상에서의 프로필렌 직접산화 반응을 통한 산화프로필렌의 제조” 2018 년 한국공업화학회 춘계학술회의, 2P-504, 대구 엑스코 (2018/5/2-4).

7. Domestic Conference (Co-Author)

1. 이윤재, 이어진, 김정권, 홍웅기, 이종협, 윤중락, 송인규, “화학적 활성화법을 이용하여 제조된 활성 카본 에어로젤-그래핀 화합물의 물리화학적 특성 및 슈퍼커패시터 전극으로서의 전기화학적 특성에 관한 연구”, 2014 년 한국화학공학회 춘계학술회의, P 촉매금-91, 창원컨벤션센터 (2014/4/23-25).

2. 이윤재, 이어진, 김정권, 홍웅기, 이종협, 윤중락, 송인규, “PEI(polyethyleneimine) 처리된 산화 그래핀을 사용하여 제조된 카본 에어로젤-그래핀 화합물의 합성 및 슈퍼커패시터 전극으로 응용: PEI 처리된 산화 그래핀의 양이 전기화학적 물성에 미치는 영향”, 2014 년 한국공업화학회 춘계학술회의, 1P-261, 제주 ICC (2014/4/30-5/2).

3. 김정권, 박해웅, 이종권, 이어진, 송인규, “전이금속 및 귀금속이 담지된 중형기공성 탄소 담체를 이용한 리그닌 모델화합물의 분해반응 및 분해경로 규명”, 2014 년 한국화학공학회 추계학술회의, P 촉매금-9, 대전 DCC (2014/10/22-24).

4. 이종원, 강태훈, 이어진, 백민성, 노영수, 송인규, “물리적 표면특성이 조절된 중형기공 카본에 팔라듐이 담지된 촉매를 이용한 과산화수소 직접 합성 반응에 대한 연구”, 2016 년 한국화학공학회 춘계학술회의, P 촉매금-46, 부산 BEXCO (2016/4/27-29).

5. 박승원, 한승주, 유재경, 송지환, 이어진, 송인규, “니켈-스트론튬-알루미나-지르코니아 에어로젤 촉매 상에서의 에탄올 수증기 개질 반응을 통한 수소 가스 생산”, 2016 년 한국화학공학회 추계학술회의, P 촉매금-35, 대전 DCC (2016/10/19-21).

6. 이종원, 강기혁, 이어진, 송인규, “산특성이 조절된 중형기공 카본에 팔라듐이 담지된 촉매에 의한 과산화수소 직접 합성 반응에 관한 연구” 2016 년 한국화학공학회 추계학술회의, P 촉매금-74, 대전 DCC (2016/10/19-21).

7. 강기혁, 한승주, 이종원, 유재경, 박승원, 이어진, 송인규, “붕소가 첨가된 Re-Ru/C 촉매 상에서 숙신산의 수소화를 통한 1,4-부탄디올의 제조” 2016 년 한국화학공학회 추계학술회의, P 촉매금-94, 대전 DCC (2016/10/19-21).

8. 박승원, 유재경, 송지환, 이어진, 유상범, 송인규, “수소가스 생산을 위해 비금속 조촉매 붕소를 도입한 중형기공성 니켈계 상에서 액화천연가스의 수증기 개질 반응을 통한 수소 가스 생산”, 2017 년 한국화학공학회 춘계학술회의, P 촉매목-4, 제주 ICC (2017/4/26-28).

9. 이종원, 강기혁, 이어진, 노영수, 송인규, “술폰산기가 도입된 중형기공 카본에 담지된 팔라듐 촉매에 의한 과산화수소 직접 합성 반응에 관한 연구”, 2017 년 한국화학공학회 춘계학술회의, P 촉매목-3, 제주 ICC (2017/4/26-28).

10. 노영수, 김민영, 이어진, 이종원, 송인규, “제올라이트 촉매 상에서 이소부탄의 알킬화반응”, 2017 년 한국화학공학회 춘계학술회의, P 촉매목-2, 제주 ICC (2017/4/26-28).

11. 박승원, 유재경, 송지환, 이어진, 유상범, 송인규, “조촉매로 몰리브데넘을 도입한 중형기공성 니켈계 제로젤 촉매 상에서 액화천연가스의 수증기 개질 반응을 통한 수소 가스 생산”, 한국화학공학회 추계학술회의, P 촉매목-1, 대전 DCC (2017/10/25-27).